

Illinois Basin–Decatur Project

Robert A. Bauer, Robert Will, Sallie E. Greenberg, and Steven G. Whittaker

Introduction

The Illinois Basin–Decatur Project (IBDP) is an integrated bioenergy carbon capture and geological storage (BECCS) project conducted at Archer Daniels Midland Company's (ADM) corn processing plant in Decatur, Illinois, USA (Figure 19.1). Over three years approx. 1000 tonnes/day of carbon dioxide (CO_2), obtained from ethanol production at the ADM plant, was compressed, dehydrated, sent along a 1.9-km pipeline, and injected into the Mt. Simon Sandstone 2.14 km deep in the Illinois Basin. Injection took place from November 17, 2011 to November 26, 2014, with 999 215 tonnes of supercritical CO_2 injected and geologically stored (Greenberg et al., 2017).

The IBDP is led by the Illinois State Geological Survey (ISGS) through the Midwest Geological Sequestration Consortium (MGSC) that includes partners Schlumberger Carbon Services, Trimeric Corporation, ADM, and other research organizations. The MGSC is one of seven regional partnerships funded by the U.S. Department of Energy–National Energy Technology Laboratory (DOE–NETL) to build capacity and gain experience in CCS through regional characterization, pilot studies, and demonstration projects. In addition to the injection operations, the MGSC has deployed a full range of surface and subsurface monitoring verification and accounting (MVA) technologies throughout each of the project phases (preinjection, injection, and postinjection) to evaluate their effectiveness for use at long-term, large-scale CCS projects, including geophysical methods.

The IBDP site includes one injection well (CCS1), one deep monitoring well (VW1), one dedicated geophysical well (GM1), and a variety of near surface monitoring wells and equipment. For MVA, a combination of continuous pressure measurements from the injection and multilevel monitoring well, continuous passive monitoring of microseismic

activity, repeat Reservoir Saturation Tool (RST)¹ logging measurements, and repeat surface and borehole seismic surveys have been used to monitor the development of pressure and CO_2 saturation throughout the project. In addition to subsurface monitoring and characterization, the IBDP MVA program included extensive soil flux, atmospheric monitoring, and shallow groundwater monitoring activities. A unique challenge related to this site is that it is at a very active industrial site that impacts significantly on monitoring activities and strategy. This chapter will focus on the geophysical aspects of site characterization and monitoring conducted at the IBDP from 2007 to 2017 (Figure 19.2).

Geological Setting and Site Characterization

Geological site characterization at the IBDP is based on examination of more than 250 m of whole core, geophysical well logs, two-dimensional (2D) and three-dimensional (3D) seismic, and a range of tests and analyses (Freiburg et al., 2014). The primary injection target of the IBDP is the Cambrian Mt. Simon Sandstone, an extensive formation that underlies much of the Midwestern United States, which is also used regionally for geological storage of natural gas. The Mt. Simon reaches its maximum thickness of approx. 790 m near the IBDP site, and is divided lithostratigraphically into Lower, Middle, and Upper sections. These major sections are further divided into units based on depositional facies interpreted using core examination and downhole geophysical logging results (Figure 19.3), and include fluvial braided river, floodplain, and alluvial plain deposits; eolian (windblown deposit) sandsheet, dune, and interdune deposits; and shallow marine deposits. The injection of CO_2 took place within a single lithological unit of

¹ Mark of Schlumberger.



Figure 19.1 Map of the IBDP site with the location of wells. The CCS1, VW1, and GM1 wells are infrastructure for IBDP. CCS2, VW2, and GM2 are similar well configurations installed for the Illinois Industrial Carbon Capture and Storage (ICCS) Project.

the Lower Mt. Simon Sandstone between 2129 m and 2138 m, where porosity and permeability range 18–25% and 40–380 mD, respectively; the reservoir interval overall has an average porosity of about 20% and an average permeability near 200 mD.

The Mt. Simon is overlain by the Eau Claire Formation, a 150 m thick impermeable package that hydraulically isolates the Mt. Simon from overlying strata (Palkovic, 2015). A 70-m shale unit in the lower part of the Eau Claire forms a highly effective seal to vertical fluid movement, and the upper portion of the Eau Claire is dense limestone with thin stringers of

siltstone. Together the Mt. Simon and Eau Claire form the storage complex at the IBDP.

Pre-Mt. Simon strata (informally known as the Argenta Formation) are in disconformable contact with the lower Mt. Simon and, although they are lithologically similar to the Mt. Simon, they have distinct depositional character and are generally well cemented and compacted throughout, resulting in significantly lower porosity and permeability (Figure 19.3). The Argenta deposits comprise the basal beds in the sedimentary succession at IBDP, and are in sharp, nonconformable contact with the

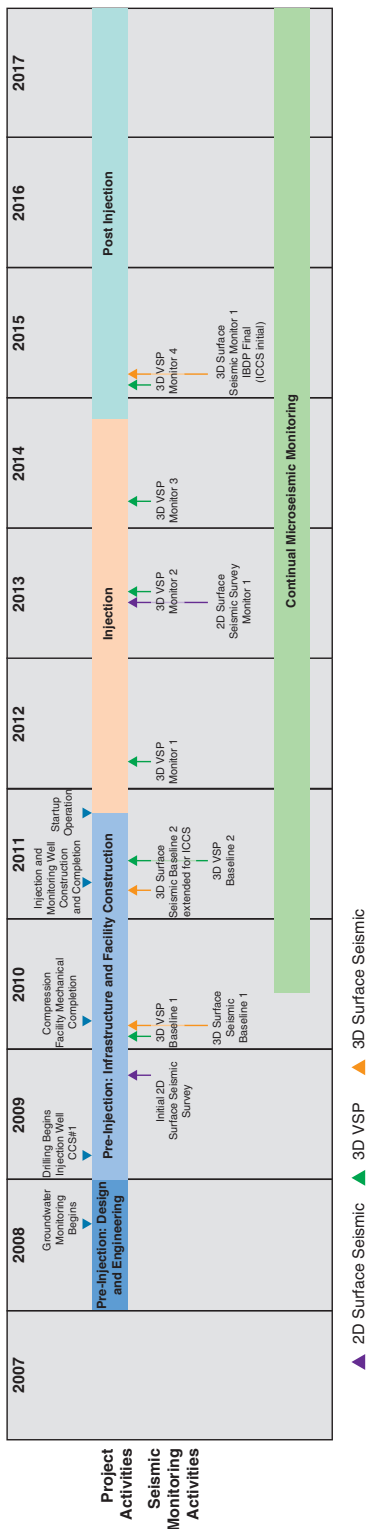


Figure 19.2 Geophysical program timeline.

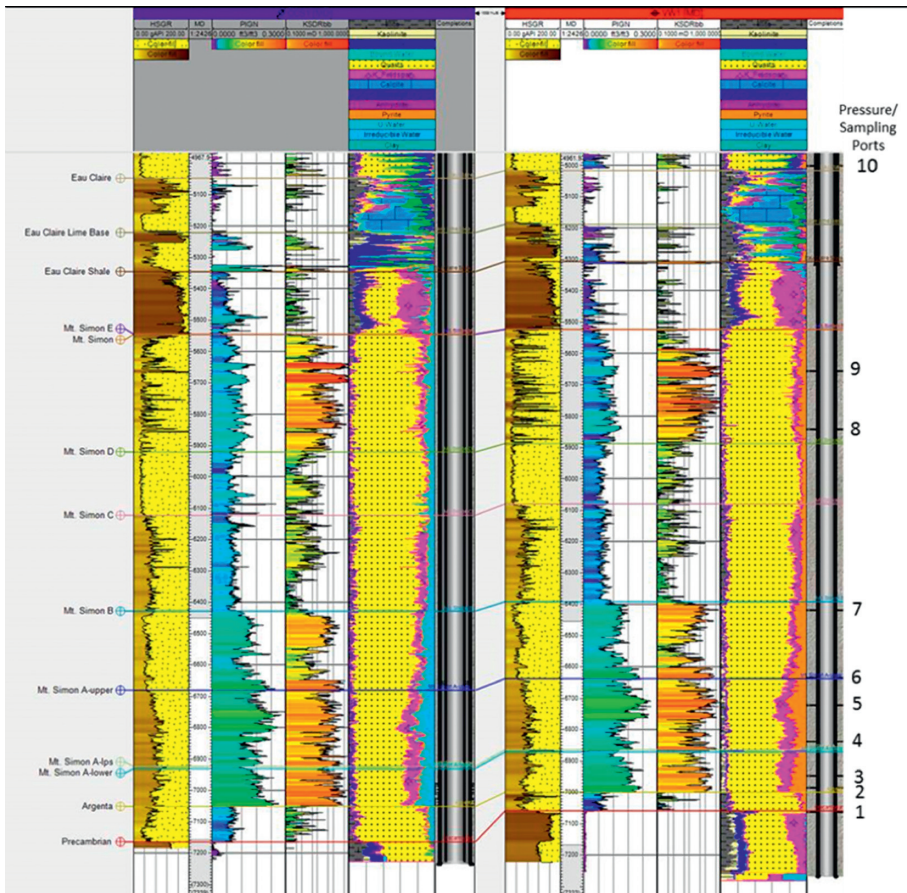


Figure 19.3 Cross section of the IBDP study site. CCS1–VW1 cross section showing the Precambrian crystalline basement, Argenta Formation (Pre-Mt. Simon), Mt. Simon Sandstone, and part of the Eau Claire Formation.

Precambrian basement. The Argenta can contain angular clasts of underlying basement rhyolite, and regional seismic data indicates more than 500 m topographic relief may exist on the Precambrian basement surface prior to Phanerozoic deposition (Leetaru and McBride, 2009). At the IBDP site, the Precambrian crystalline basement is layered rhyolite over granodiorite over granite, as shown by sidewall cores and geophysical logs (Bauer *et al.*, 2016). The basement rock can be highly fractured showing mineralization, slight alterations along the cracks, or a combination of both (Haimson and Doe, 1983).

The bedrock strata in the region of the IBDP site exhibit a slight dip of approx. 1° to the southeast, and the closest structures to the site (Figure 19.4) are minor anticlines with small structural closure about 40 km south and 30 km north.

Subsurface Configuration

The subsurface components of the IBDP geophysical site characterization and monitoring network are deployed in three multipurpose wells; the injector CCS1 (Figure 19.5), the deep verification and monitoring well VW1 (Figure 19.5), and the geophysical monitoring well GM1 (Figure 19.6). In addition to its primary function of injecting supercritical CO₂ into the Lower Mt. Simon, CCS1 hosts downhole pressure and temperature gauges, primary elements of the IBDP passive seismic monitoring array, and was an access for repeat geophysical logging, all of which are key components of the MVA program. The VW1 well, although not hosting seismic measurements, provided 11 pressure measurement and fluid sampling ports throughout the geological column extending from the Precambrian

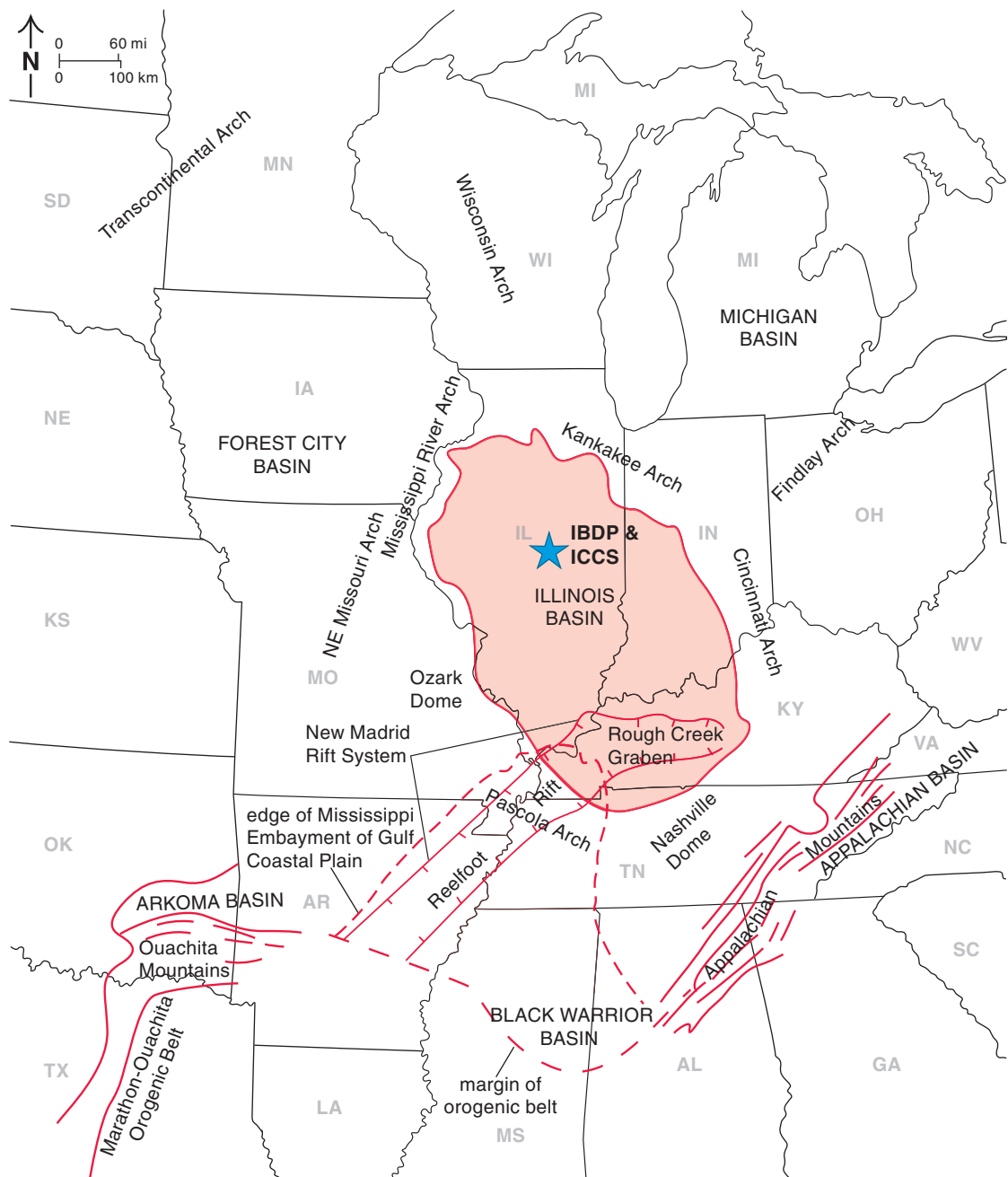


Figure 19.4 Regional fault map. The map shows regional faults with the location of the Illinois Basin (pink shaded area) and the IBDP site (blue star).

to the Underground Source of Drinking Water (USDW).² In addition, VW1 also was accessed for repeat geophysical logging. The GM1 well, originally intended to facilitate repeat 3D vertical

² The VW1 well was originally completed with a Westbay pressure/temperature and fluid sampling system. At the time of this writing, the VW1 well has been recompleted with a different monitoring system not described herein (section “Pressure Monitoring”).

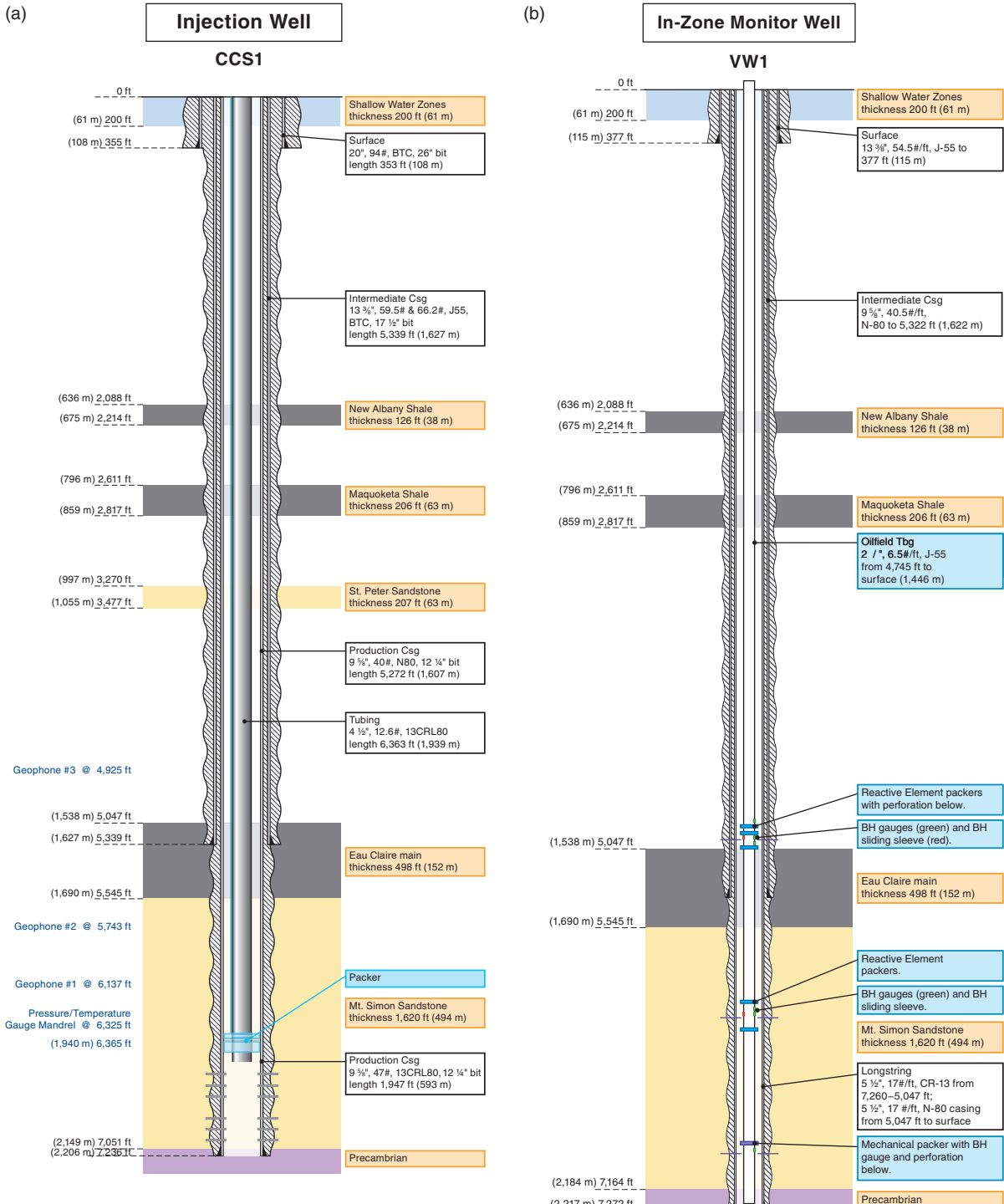


Figure 19.5 Schematic of the injection well CCS1 and deep monitor well VW1.

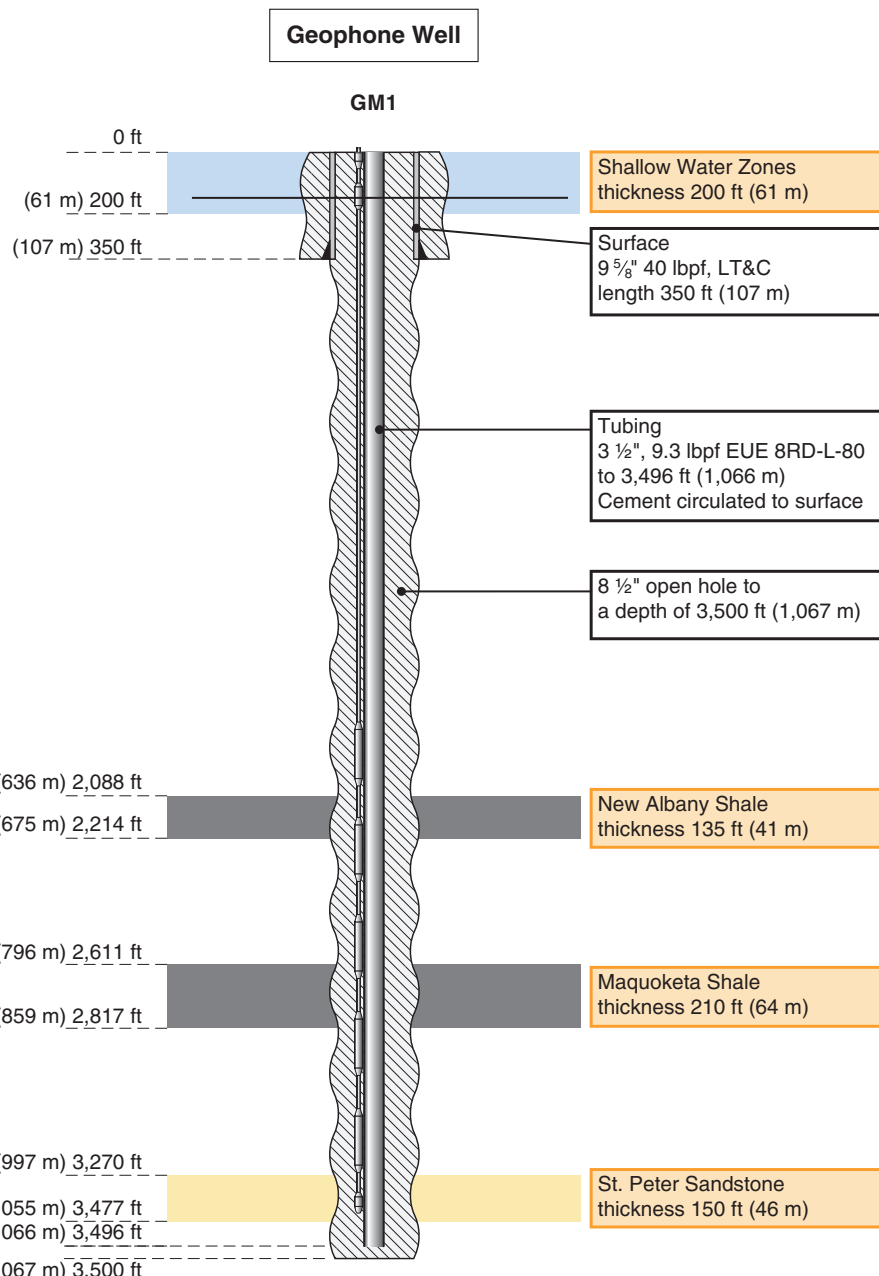


Figure 19.6 Schematic of geophysical monitoring well GM1.

seismic profile (VSP) data acquisition, is also a vital component of the passive monitoring network. The specific equipment descriptions

and roles of each well will be elaborated on in the following sections on respective geophysical methods.

Geophysical Methods and Data Acquisition Programs

Overview

The IBDP geophysical program has provided valuable direct and indirect measurements of key elastic and petrophysical properties for characterization of the injection zone, seal, and underlying formations. A systematic geophysical site characterization effort started with acquisition of 2D seismic data to support pre-drill feasibility assessment. The site characterization was progressively refined through drilling and geophysical logging of the injection and monitoring wells, and acquisition of surface and borehole three-dimensional (3D) seismic surveys. The program entailed systematic improvement of spatial coverage and measurement resolution as the project progressed. Site characterization also included establishment of the background microseismic activity through 18 months preinjection passive monitoring.

The IBDP site characterization and monitoring program includes a combination of permanent and retrievable borehole and surface measurement techniques to acquire data both continuously and periodically. Various geophysical methods are required to estimate intrinsic properties of the storage complex for site characterization and to monitor transient reservoir state (pressure, saturation, stress) for MVA purposes. The field configuration and methodology have evolved throughout the project to achieve the best solutions to multiple technical challenges under ever changing operational and commercial conditions and constraints. The following sections describe each element of the site characterization and monitoring system. Other chapters in this book (particularly Chapter 2) provide more detail on the fundamentals of the methods used at the IBDP.

Active Seismic Methods

2D Surface Seismic Data

Before commencement of the IBDP geophysical data acquisition campaign, preexisting regional 2D seismic data were the primary source of structural information for pre-drill site characterization. Two 2D seismic profiles (ADM1 and ADM2) were acquired along the east–west and north–south roads that pass by the ADM plant in the fall of 2007. These data, along with

nearby wells, were used to reduce project risk associated with reservoir thickness, potential faulting, and storage capacity at the site. As a result of positive preliminary assessment of the area, an additional four 2D seismic data lines were acquired at the site in 2009 to obtain additional geological detail and supplement pre-drill planning. The seismic data acquisition program for site characterization is described in Table 19.1. New data further verified the absence of significant basement paleotopographic highs at the site and a very thick Mt. Simon section. These data also supported estimates of local regional trends during site characterization and development of the 3D reservoir model (Leetaru and Freiburg, 2014).

3D Surface Seismic Data

The IBDP site characterization and monitoring program involved three separate surface 3D seismic data acquisition efforts (Table 19.1). The first 3D survey conducted in 2010 was designed for detailed site characterization over the anticipated CCS1 plume area. In 2011, this survey was extended to accommodate potential additional plume monitoring needs. This extended survey (2011) also served as the baseline survey for subsequent IBDP time-lapse monitoring work. The third survey, conducted in 2015, was after completion of injection of CO₂ and this survey serves as the first time-lapse monitor survey for the IBDP plume.

Acquisition of the 3D surveys at the IBDP presented many evolving challenges. The proximity of heavy industrial activity and transportation infrastructure resulted in high levels of anthropogenic noise. New construction at the industrial site meant that each successive survey encountered additional obstructions to access and related increase in noise. The requirement to acquire surveys during the winter season owing to both agricultural activity and desirable ground coupling conditions further compounded the difficulties. The resulting progressive diminishment of achievable surface access, the accompanying progressive increase in levels of noise contamination due to surface industrial activity, and an electrical power infrastructure onsite created challenges to seismic data acquisition. These acquisition challenges were managed through a combination of acquisition design, equipment, and parameter selection. For example, the 2D seismic data was used to determine the potential frequency bandwidth and resolution of

Table 19.1 Seismic data acquisition program components

Date	Data	Purpose and comments
2007	Review of existing regional geophysical data	Increased understanding of regional geology Relatively poor quality Not site specific for project
October 2007	Two 2D seismic profiles (IA17 and IA 27)	Refined understanding of project site and regional geology
December 2009	Four high-resolution 2D seismic profiles	Validated regional dip from previous interpretations Provided confirmation that no resolvable faults were present Contributed to the understanding of local geology
January 2010	High-resolution 3D surface seismic survey	Provided detailed structural and stratigraphic characterization Used to derive rock properties for the Eau Claire and Mt. Simon
January 2011	High-resolution 3D surface seismic survey	Merged with 2010 survey to increase the seismic data coverage for structural and stratigraphic characterization; includes the ICCS Project site
January 2015	High-resolution 3D surface seismic survey	Served as postinjection time-lapse monitor survey for the IBDP and baseline survey for the ICCS Project

the new 3D seismic data set, which showed that it was feasible to acquire a high fold 3D surface seismic survey over the site despite the access limitations. However, some of the pre-survey source and receiver positions were lost once the acquisition crew started work in the field because of ground conditions and changes in infrastructure related to the industrial site. The acquisition crew worked with the survey design team to adapt the survey where surface access was an issue to ensure high fold coverage was maintained. As a result, the final post-survey fold coverage was very similar to the ideal pre-survey fold coverage. Acquisition design at the IBDP is discussed in detail by Couëslan *et al.* (2009).

The Schlumberger Q-Land point-receiver land seismic system was used at the IBDP, which incorporates a pattern of high-density, high-resolution 18-Hz geophone accelerometers. This acquisition configuration was intended to give the maximum amount of flexibility in attenuating the high levels of noise contamination at this industrial site, while maintaining high-frequency bandwidth during processing. The 27 216 kg vibrator trucks used a maximum displacement sweep design to generate energetic low frequencies from 4 to 100 Hz to maximize the low-frequency content in the dataset. Seismic data with frequencies between 2 and 10 Hz are particularly useful for inversion analysis, as they

can build a more robust low-frequency model less biased by sparse well-log data.

Although under ideal circumstances exact repeatability is desired in all aspects of time-lapse seismic surveying, unavoidable events result in variations in recording equipment between surveys. By maintaining consistent high-density single-receiver locations, together with specially designed vibrator sweeps, both signal and noise modes provided the fidelity required for noise reduction in data processing. The data acquisition parameters, which were maintained throughout all 3D surveys, are shown in Table 19.2. The source and receiver locations used for the 2015 time-lapse monitor survey are shown in Figure 19.7a. All of these source and receiver locations are redundant with those occupied in the 2011 survey. The fold of coverage on the processing bin size achieved in the 2015 survey within the offset limited range of 2135 m corresponding to target depth is illustrated in Figure 19.7b. The uniformity of common depth point (CDP) coverage in light of the numerous surface obstructions demonstrates the power of high-density source and receiver effort.

Borehole Seismic: Vertical Seismic Profiles

Time-lapse 3D vertical seismic profiles (VSP) were an important component of the MVA plan for the IBDP.

Table 19.2 3D surface seismic data acquisition parameters

Recording parameters	
Recording system	Variable
Recording format	SEG-D, IEEE
Record length	5 s
Sample rate	2 ms
Recording filter (Hi-Cut)	100 Hz
Recording filter (Low-Cut)	4 Hz
Nominal fold	60
Receiver type	GAC-C
Line geometry	Detector interval = 10 ft.
Source Parameters	
Source	Vibroseis
Source type	AHV IH 67 000 lbs.
Shotpoint interval	80 ft.
Sweep number	4
Sweep start frequency	4 Hz

Time-lapse VSPs were intended to provide information on CO₂ plume development, demonstrate containment of the CO₂ in the storage formation, and provide data to verify and update models and simulations over the life of the project (Couëslan *et al.*, 2013). The VSP array was permanently cemented into GM1 – the dedicated geophysics monitoring well located approx. 60 m northwest of the injection well. The array consisted of 31 levels of 3C phones deployed at depths ranging from approx. 50 m to 1050 m below ground surface.

Six 3D VSP surveys were acquired at the site: two baseline surveys and four monitoring surveys (Table 19.3). Although borehole deployment of the receiver array, combined with the much-reduced energy source footprint, resulted in fewer access problems than encountered during surface seismic acquisition, the relative contribution of each VSP source point to the final image is much greater in VSP surveying. As such, surface access was a major challenge to achieving repeatability between successive VSP surveys. The VSP acquisition conditions, source parameters, and quantity of CO₂ injected for each survey are summarized in Table 19.3.

Given the use of a permanent receiver array, the greatest remaining challenge to successful time-lapse imaging is in achieving repeatability of energy

source point locations. This was particularly problematic at the IBDP site where permitting issues resulted in restricted access to major sections of the surface for the first three monitor surveys. The resulting reduction in source points resulted in reduction of image quality for these surveys and also in low-resolution time-lapse signals from these monitor surveys. Monitor 4 overcame some of the restrictions to surface access and Figures 19.8a and 8b show source and receiver location analysis for the Baseline 2-Monitor 4 (B2-M4) survey set. Green polygons in Figure 19.8a delineate the shotpoints not accessible during M1, M2, and M3 surveys. This, together with greater quantity of injected CO₂, is believed to be a major factor in the enhanced stability of time-lapse analysis for the B2–M4 survey pair (Section 5.2.1).

Passive (Microseismic) Monitoring

System Overview

The IBDP microseismic monitoring network is comprised of multiple subsurface arrays deployed in three separate wells. The subsurface data acquisition network components are described in Table 19.4. The arrays in CCS1 and GM1 were calibrated using drilling noise and perforation shots in the borehole of VW1, which Smith and Jaques (2016) describe in detail.

Data from all subsurface arrays are integrated and real-time data acquisition functions are performed using an integrated data acquisition system located at the field office. In addition to the subsurface equipment, ISGS installed five surface seismometer stations (Figure 19.9). The raw microseismic data stream from the subsurface array is recorded in 10-s SEG2 files. The rate of data sampling during the preinjection period was every 2 ms (500 samples per second). The data set composition is described in terms of date ranges, number of files, number of triggers, and events identified. The number of triggers represents the total number of possible events detected by the system, and so includes many false triggers. Given the sensitivity of the system, false triggers are caused by any combination of transient electrical glitches and well-related activity such as pipeline maintenance. A false trigger will not have a P- and S-wave signature common to microseismicity or place an event in the subsurface.

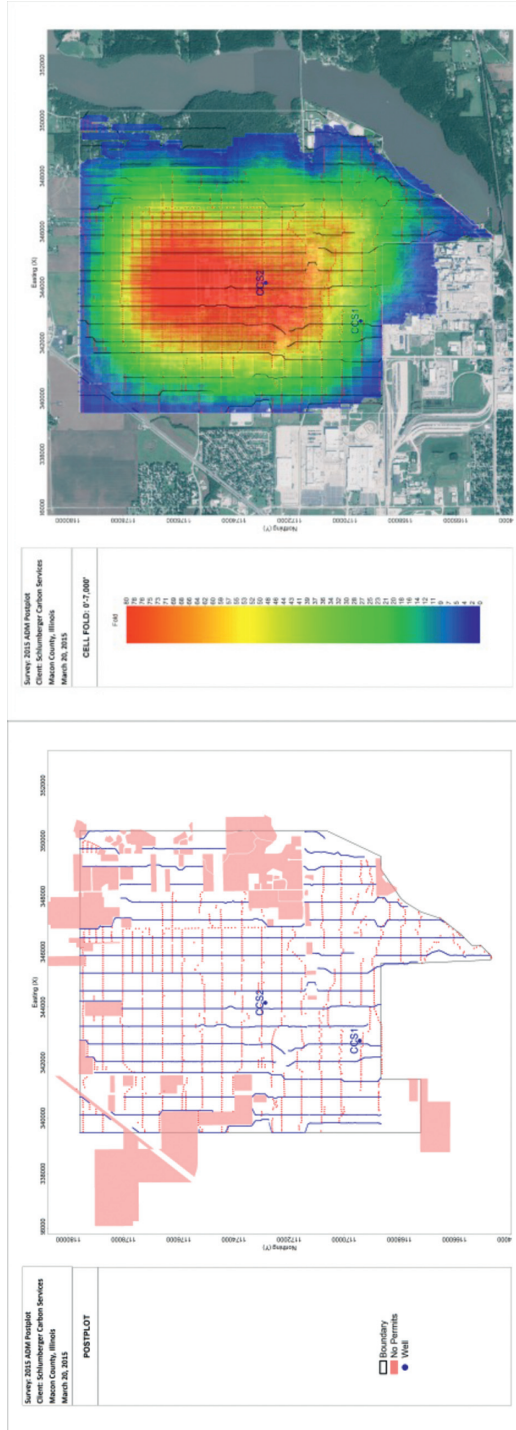


Figure 19.7 Seismic source and receiver locations with fold coverage. (a) 2015 monitor survey source and receiver postplot with surface obstructions (shaded red) and (b) resulting fold of coverage on processing bins and limited to 2135 m.

Table 19.3 Schedule of time-lapse VSP surveys and injected CO₂ quantity.

Survey	Date	Ground conditions	Vibrator sweep (Hz)	Repeated shots (relative to B2)	Amount of injected CO ₂ (tonnes)
Baseline 1 (B1)	Jan. 27–30, 2010	Wet	2–100	—	Preinjection
Baseline 2 (B2)	Apr. 12–14, 2011	Dry	8–120	—	Preinjection
Monitor 1 (M1)	Feb. 11–12, 2012	Frozen/Dry	8–120	467	74 000
Monitor 2 (M2)	Apr. 4–5, 2013	Damp	8–120	385	433 000
Monitor 3 (M3)	Feb. 3–5, 2014	Frozen	8–120	378	730 000
Monitor 4 (M4)	Jan. 15–17, 2015	Frozen	8–120	458	approx. 1 000 000

Geophone Arrays

Injection Well (CCS1)

In the original monitoring plan, the passive seismic monitoring equipment in CCS1 was anticipated to provide the majority of the observations for microseismic location and characterization (Figure 19.5). A specialized deployment mechanism was used to decouple the sensors from the injection tubing string, thereby reducing flow-induced noise. As originally designed, the four sensor levels in CCS1 were set at subsurface depths spanning the interval from the Eau Claire to Unit A of the Mt. Simon (deepest part of the formation), which was intended to provide reasonable signal fidelity and location accuracy throughout the primary seal and injection intervals. Damage to two sensors during deployment resulted in only the two sensors located nearest the injection zone being usable. The eight channels of data from these two sensors are recorded via the 96-channel DAU located at the nearby field office. Preinjection data acquisition began in May 2010.

Geophysical Monitoring Well (GM1)

The dedicated geophysical monitoring well, GM1, is 1067 m deep and contains a 31-level array of 3-component tools permanently cemented into place (outside the casing) during construction (Figure 19.6). The geophones are approx. 500 m shallower than those in CCS1, and 29 of the geophones are located between 623 and 1049 m depth with the remaining two at 41 and 108 m (Will *et al.*, 2016a).

The primary objective of the GM1 array was to obtain high repeatability time-lapse 3D VSP surveys for plume monitoring. The main well construction and array design considerations focused on VSP imaging objectives, with secondary objectives to support

microseismic monitoring. However, given the reduction of observations in CCS1, as mentioned earlier, the significance of observations from the GM1 array for microseismic characterization greatly increased. Data recording in GM1 also commenced in May 2010. Data from a selected 28-level (86-channel) subset of the 31-level array are recorded to the 96-channel DAUs, along with data from CCS1.

Geophones Orientation

Locating microseismic events requires precise knowledge of the position of the geophones in *x*, *y*, and *z* directions, and the orientation of the geophones within that position.

Tool orientation calculations were performed on the various IBDP subsurface arrays at different times during the monitoring project as new subsurface components were added and energy sources became available because of field activities. Because the array in CCS1 provides the primary observations constraining the azimuth used in calculating microseismic event locations, verifying accurate orientation of these geophones was attempted during all orientation efforts.

Surface Passive Monitoring Stations

In 2013, a network of five 3-component seismometers were installed in shallow, near-surface vaults on ADM property and away from buildings (Figure 19.9). Four of the surface seismic stations were deployed in approximately the four cardinal directions from the CCS1 well at radial distances of 1066.8 to 1828.8 m. The fifth station is located outside the National Sequestration Education Center building at Richland Community College (labeled as Seis3 RCC in Figure 19.9) where real-time data monitoring is

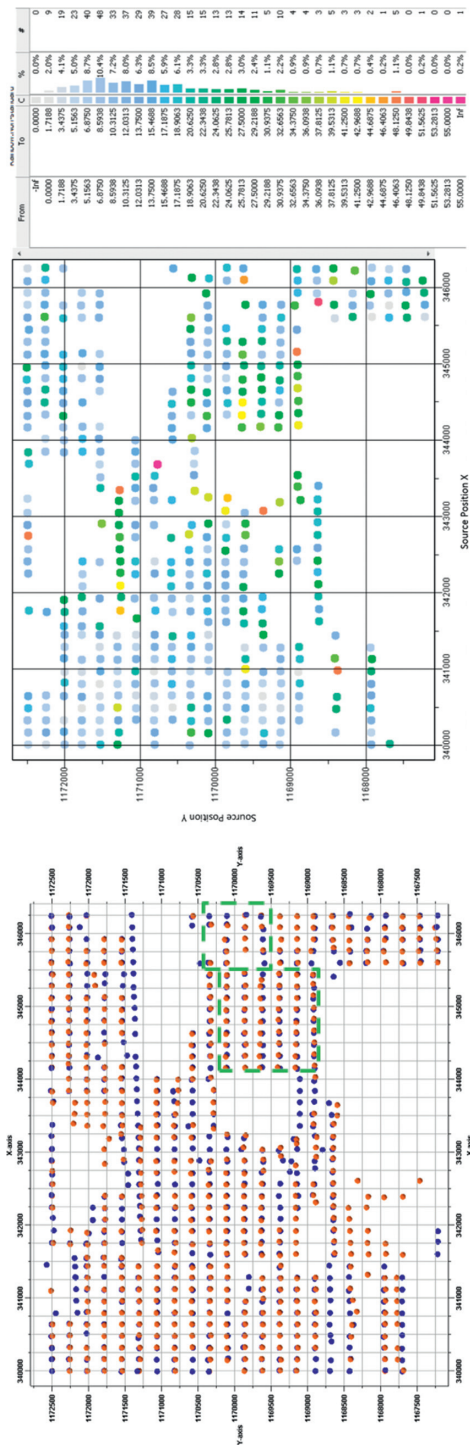


Figure 19.8 VSP source and receiver locations. (a) Source locations from B2 and M4 surveys. Orange dots are B2 and Blue are M4 shot points. Green boxes show the shots that were not available in M1, M2, and M3 surveys. (b) Extracted collocated sources, survey B2com4. The color of circles indicated the relative distance from the corresponding source location from M4 survey.

Table 19.4 Microseismic system components

Well	Configuration	Recording
CCS1	2-level array of a 4-component WellWatcher PS3* passive seismic sensing system with 4-Geospace 2400 geophones in tetrahedral configuration (two levels functioning)	96-channel data acquisition unit (DAU) located at the field office near CCS1
GM1	A 31-level array of 3 Geospace 2400 geophones in orthogonal configuration	96-channel DAU located at the field office near CCS1
VW2: Operated by the ICCS Project	5-level array of a 3-component multilevel downhole seismic array, Sercel array installed temporarily (Sept. 26, 2013 and removed Feb. 25, 2015)	24-channel DAU located at the wellhead

**Figure 19.9** Location of five surface seismometers at the IBDP site.

performed for this station. This near-surface network was intended to be a backup for the downhole microseismic systems for large magnitude events. The instruments in the near-surface system will continue to record on-scale if a seismic event, large enough to saturate the downhole microseismic systems, were to occur near the IBDP site. If a large event were to occur, the sensors in the downhole systems would be able to detect the event and determine its 3D location, although they may not accurately measure the event magnitude. Though the near-surface data are not integrated with downhole data in event

processing, the data have been used for independent verification of larger events.

Nonseismic Measurements

Geophysical Logging

A comprehensive suite of geophysical logs were acquired in boreholes CCS1, VW1, and GM1, along with physical borehole and core tests in CCS1 and VW1. In addition to measurements required for geological characterization, the logging program was designed to support advanced geophysical and geomechanical integration workflows. Elastic properties, mineral fractions, and fluid saturations were measured or computed for seismic inversion and time-lapse integration. For geomechanical characterization and microseismic analysis, *in situ* stress and direction were documented by observation of tensile-induced drilling fractures and breakouts as shown by the Formation MicroImager (FMI)³ fullbore formation microimager and a minifrac, injection and step rate tests. Some of the specialized well logs, tests, and resulting measured and calculated properties used for geophysical integration at the IBDP are shown in Table 19.5.

Repeat Pulse Neutron Logs (RST)

RST logging at IBDP was performed for operational and verification monitoring; CCS1, VW1, and GM1 are logged at least annually to verify the mechanical integrity of each well. The logs are also used to monitor the development of the CO₂ plume adjacent to CCS1 and VW1 and to constrain the dynamic reservoir modeling. Two baseline surveys were acquired in CCS1 and VW1; one shortly after each well was drilled

³ Mark of Schlumberger.

Table 19.5 Petrophysical logs run in boreholes with measured and calculated properties.

Petrophysical logging tests	Measured and calculated properties
Spontaneous potential	Density
Neutron porosity	Clay content
Resistivity	Static Young's modulus
Microresistivity imaging	Static Poisson's ratio
Sonic velocities	Static shear modulus
Elemental capture spectroscopy	Biot's coefficient
Natural gamma ray	Frictional angle
Magnetic resonance	Tensile strength
Thermal neutron decay	Unconfined compressive strength
Fullbore formation microimager*	Overburden stress Minimum horizontal stress Maximum horizontal stress Azimuth minimum horizontal stress Tensile-induced drilling fractures and breakouts Mineral fractions Fluid saturations

* Mark of Schlumberger.

and a second some months after to give the drilling fluids a chance to migrate away from the wellbores.

Pressure Monitoring

VW1 was originally completed with a multilevel Westbay monitoring and sampling completion system optimized specifically for CCS applications and depth of operation. The Westbay system completion continuously monitored pressure and temperature using the Modular Subsurface Data Acquisition System (MOSDAX™, Westbay Instruments, North Vancouver, British Columbia) modular subsurface data acquisition system probes at 11 different depths in the well. Each sampling zone was isolated from the other ports through redundant packers (Figure 19.5). Fluid samples were also taken from each port at discrete time intervals for geochemical analysis when the pressure and temperature probes are pulled from the well.

Results

Surface Seismic Data

Imaging for Site Characterization

The main processing objectives for the 2010 and 2011 3D seismic surveys focused on site characterization. Processing flows were designed for

- Merging the 2011 extension with the 2010 survey
- Producing a data set suitable for acoustic and elastic impedance inversion
- Producing a volume suitable for structural interpretation
- Imaging any faults or fractures in the zone of interest (0.8–1.1 s)

The main data processing challenge for the surface 3D data set was the significant amount of random noise due to coupling issues and from anthropogenic activity, mainly roads throughout the acquisition area. Unfiltered prestack migrated gathers in Figure 19.10a illustrate the extent of noise contamination. The same gathers after a series of premigration filtering processes designed to maintain frequency and phase integrity of coherent signals are shown in Figure 19.10b. The corresponding stacked sections in which imaging is greatly improved throughout the vertical section are shown in Figures 19.11a and 11b.

Time-Lapse Processing

Data Processing

The 2011 and 2015 surveys were reprocessed for four-dimensional (4D) time-lapse detection purposes. As discussed, although it is desired to maintain identical acquisition parameters for time-lapse surveys, many factors affect acquisition such as changes of surface accessibility, random noise patterns, and changes in ground conditions. To reveal the true 4D difference caused by CO₂ injection in seismic datasets, it is important to remove other inferences as much as possible. Both the baseline and monitor datasets at IBDP were processed (coprocessed) using the same processing sequence (Figure 19.12). For several key steps, such as refraction tomography statics solution, residual reflection statics solution, and deconvolution, tests were run for both a joint solution and a standalone solution. Also, throughout processing, 4D quality control (QC) procedures were conducted to ensure non 4D

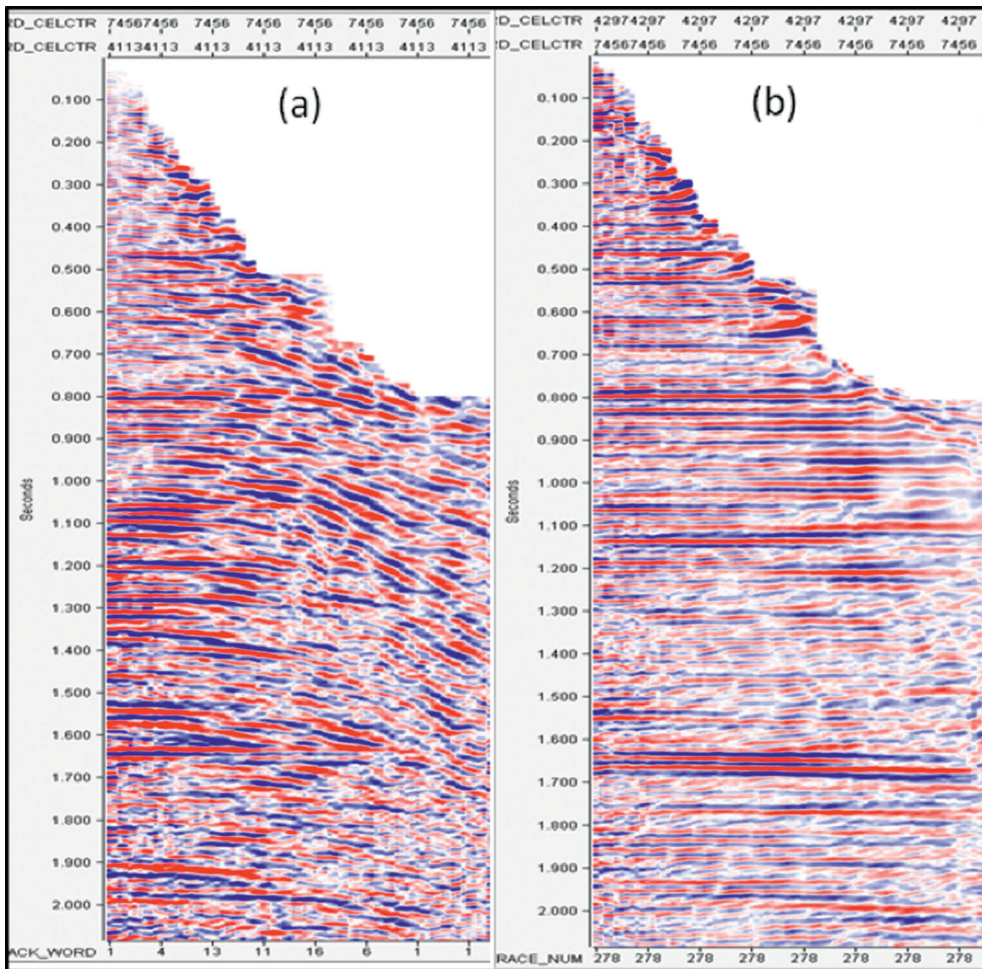


Figure 19.10 Prestack migrated 2011 3D seismic gather. Prestack migrated seismic gathers from before (a) and after (b) multichannel filtering.

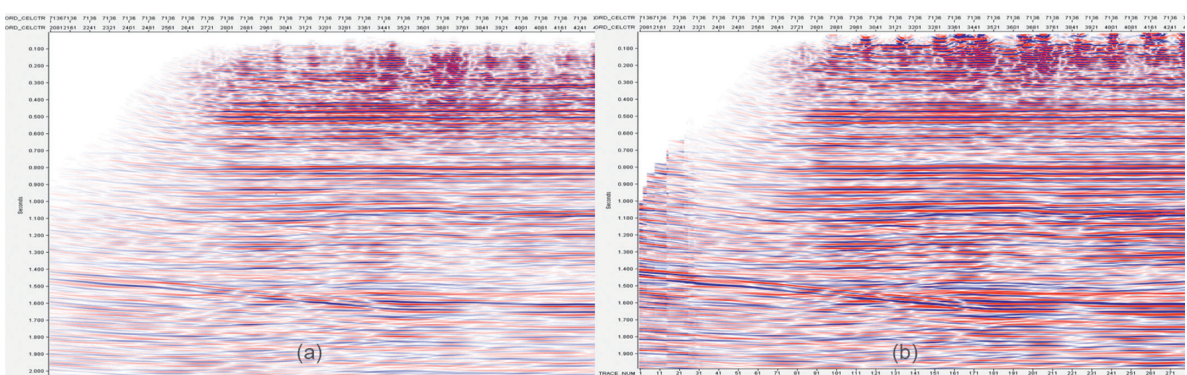


Figure 19.11 Stack 2011 3D seismic gather. Stack before (a) and after (b) multichannel filtering from gathers corresponding to Figure 19.10.

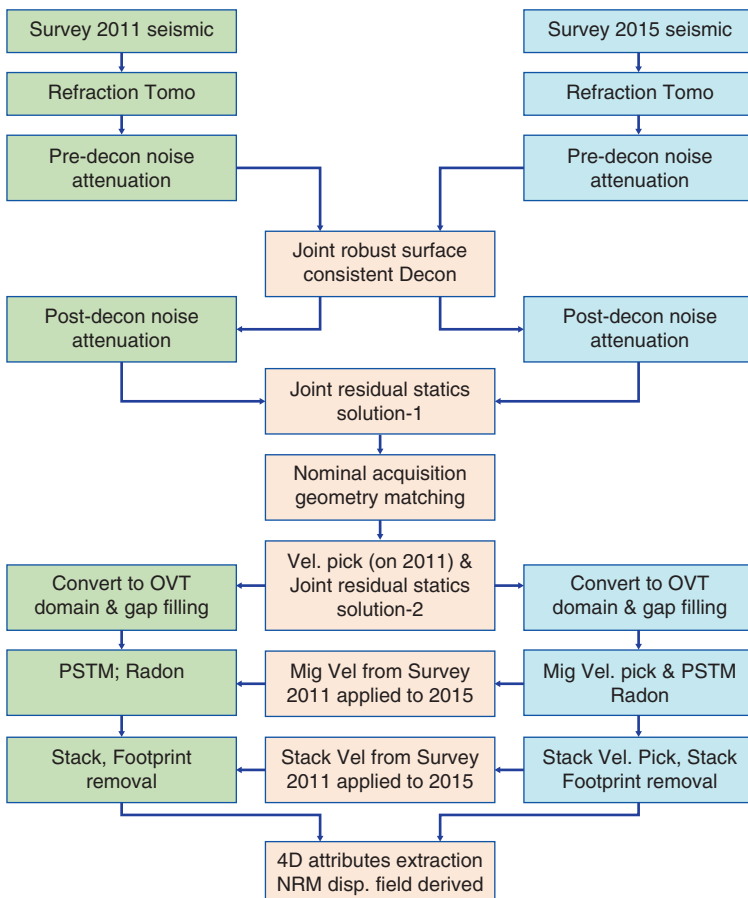


Figure 19.12 4D surface seismic data processing flow.

inferences were reduced as processing progressed. Because of the processing workflow, very subtle changes in migrated data (Figure 19.13) can be identified that are the result of time-lapse attribute analysis.

Time-Lapse Attribute Extraction

Two time windows were defined for 4D attribute extraction at IBDP (Figure 19.14). It is assumed that strata within the time Window-1 (400–700 ms) above the caprock should not be affected by CO₂ injection. Strata within the time window-2 (900–1300 ms) that includes the CO₂ injection zone could be impacted in several ways.

Replacement of one fluid by another with different density/properties changes the velocity and density of the reservoir interval, resulting in modification of reservoir acoustic impedance and/or causes small changes in reflector timing beneath the reservoir. Pore pressure changes also modify the seismic velocities within the reservoir, resulting in modification of

reservoir acoustic impedance and/or causes changes in reflector timing beneath the reservoir. Pore pressure changes may also cause gas dissolution or exsolution, producing a large change in acoustic impedance, or cause stress changes above, and possibly below, the reservoir; producing a change in velocity causes time shifts between time-lapse volumes below the reservoir.

These changes to the storage system could be detected through examination of characteristics of seismic data, and 4D attributes extracted from seismic stack volumes. Time-lapse attributes such as reliability (Figure 19.15) and normalized root mean square (NRMS) (Figure 19.16) were extracted from different time windows and were compared to detect any 4D changes caused by CO₂ injection. In both cases, the attributes from window 1 (above the injection zone) indicate good time-lapse repeatability while those from window 2 (including the injection zone) show very similar time-lapse differences, which are attributed to fluid replacement.

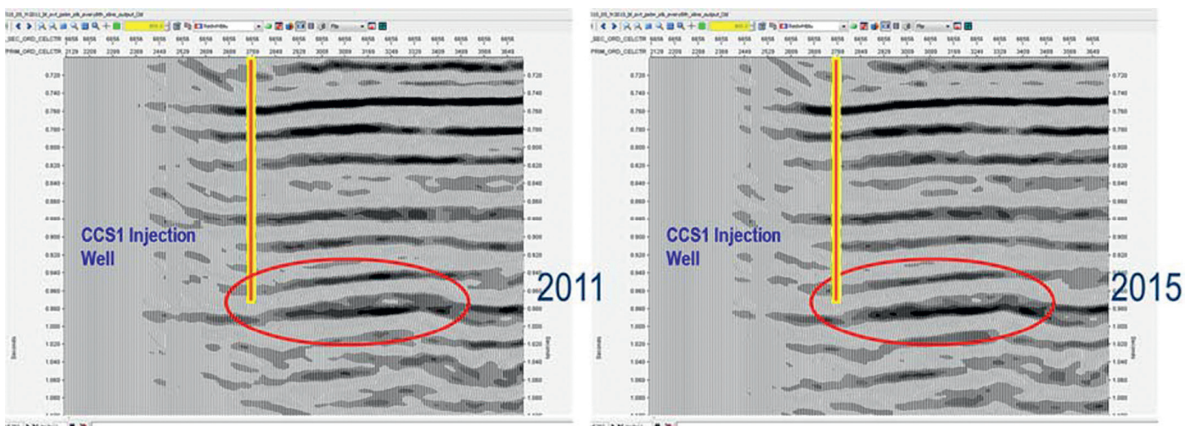


Figure 19.13 Subtle changes in migrated data. Zoom-in proximity of CO₂ injection spot (yellow bar indicates the injection well path). Notice the very subtle changes in amplitude and waveform in seismic.

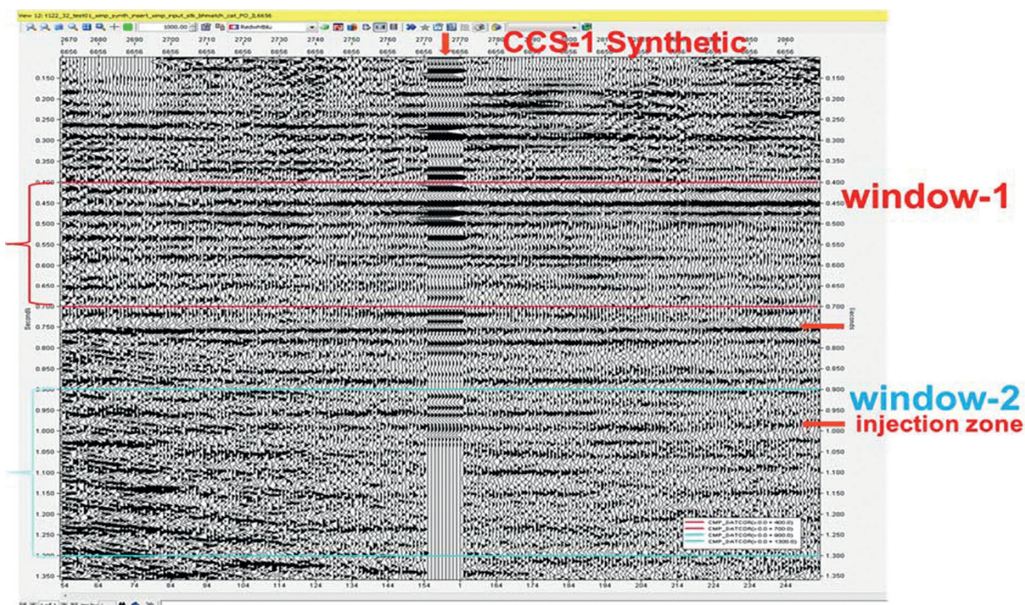


Figure 19.14 Survey 2011, 4D attribute extraction window definition. Window-1, above the CO₂ injection zone; Window-2, including the injection zone.

An additional time-lapse interpretation tool is the nonrigid matching (NRM) attribute. An NRM uses a nonrigid matching method time- or depth- to align two cubes of seismic data by generating a 3D displacement field that compares the input data to a reference volume. Owing to the fluid effect on velocity we

expect the NRM attribute to show anomalies below the plume where arrival times have been impacted by the overlying fluids. The NRM computed using the 2011 baseline survey as the reference volume is shown in Figure 19.17. An NRM anomaly in the vicinity of the injection well is clearly evident.

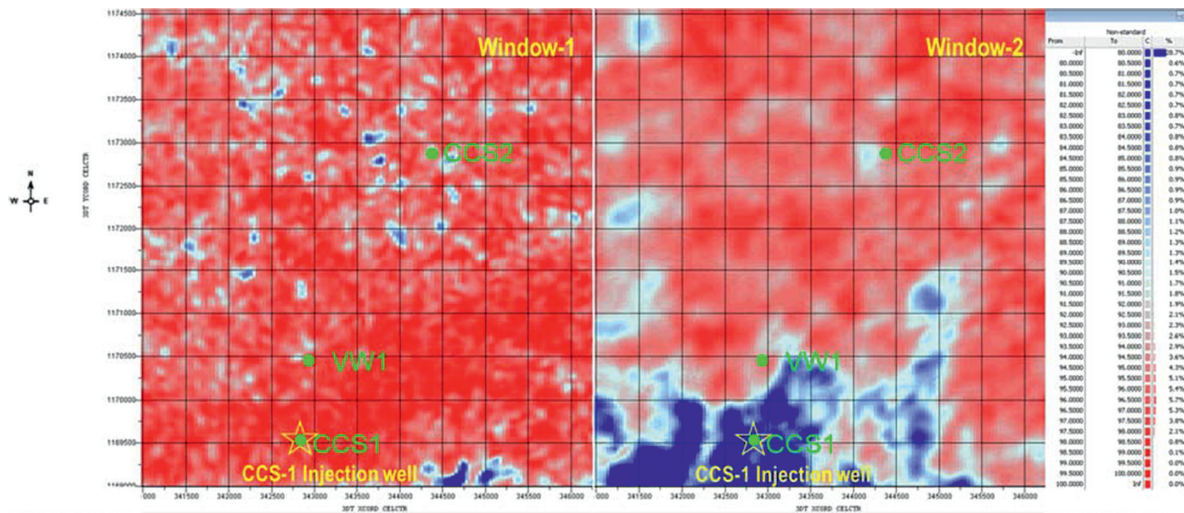


Figure 19.15 Attribute predictability comparison. Red indicates high similarity. Blue indicates low similarity.

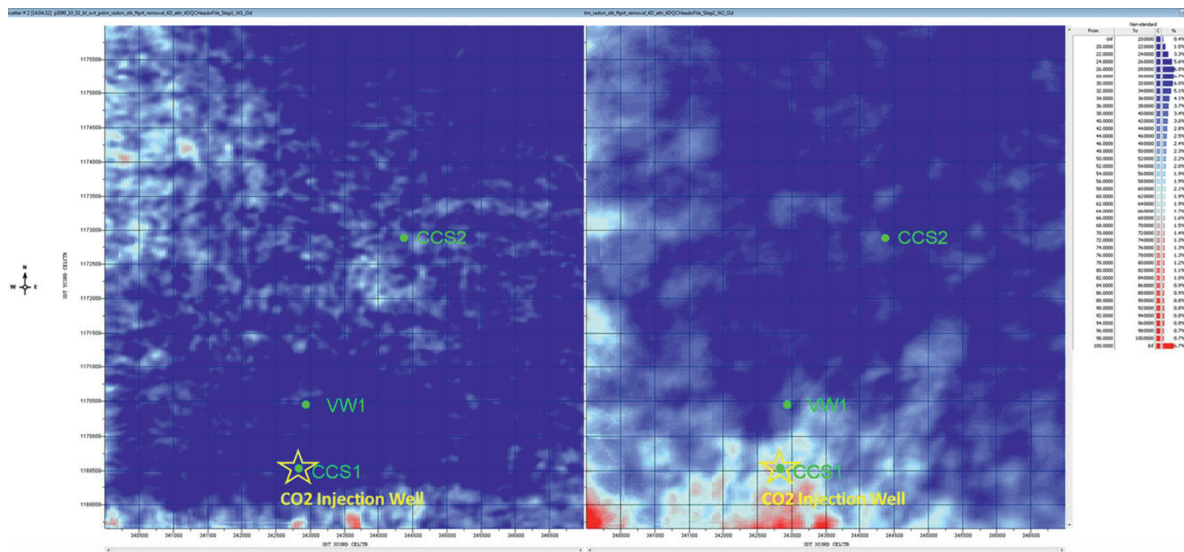


Figure 19.16 Attribute normalized root mean square comparison. Red indicates large difference in amplitude. Blue indicates small difference in amplitude.

3D VSP

Vertical Component VSP Analysis

Baseline Surveys

The first baseline 3D VSP was acquired in February 2009, after the 3D surface seismic survey, but while ground conditions were damp and not ideal

for seismic signal propagation. In addition, there was significant 60-Hz noise from nearby electrical sources, such as power lines and an electrical substation, recorded in the data although this noise was attenuated through processing. The acquisition footprint of the baseline 3D VSP also suffers from the same challenges posed by surface infrastructure obstructions to

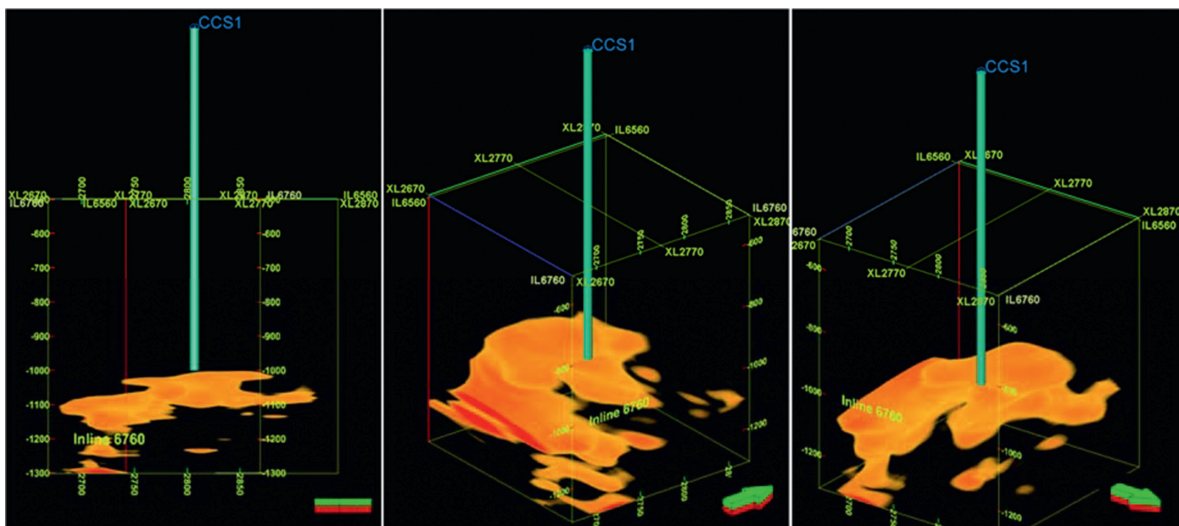


Figure 19.17 3D NRM displacement field zoomed in near the CCS1 injection zone.

energy source points. Holes in the acquisition footprint surface seismic data can be compensated by adding in-fill source and receiver locations; however, 3D VSP data is not as flexible given the geometry of the ray paths. As a result, there are identifiable artifacts in the 3D VSP images related to holes in their acquisition footprint. In 2011, a second baseline 3D VSP survey was acquired under dry ground conditions, and an isolation transformer with a Faraday shield was used to reduce the 60-Hz noise.

Monitor Surveys

Because of the favorable acquisition conditions of Baseline 2, all monitor surveys were collocated and coprocessed relative to Baseline 2 through a vertical component processing workflow (Figure 19.18). Preprocessing included receiver selection, 60-Hz notch filter, cross-equalization based trace-by-trace amplitude scaling, linear radon transform for wavefield separation, deterministic shot-by-shot reference trace wave-shape deconvolution. Collocated energy source records (15 m tolerance) were cross-equalized to allow for residual matching of the amplitude and phase spectra, and then processed for wavefield separation and VSP deconvolution. The same 1D anisotropic model that was built using zero offset VSP and 3D VSP travel times from the baseline survey was used for imaging both the datasets (Figure 19.19). After migration, nonrigid matching was applied to

both data sets to further reduce the differences between the data sets related to noise and acquisition artifacts while maintaining the differences related to CO₂ injection.

Time-Lapse Attributes

Analysis of time-lapse VSP data utilizes many of the same tools as are used for analysis of surface timelapse data. Results from the Monitor 1 and Monitor 2 surveys were ambiguous, likely from a combination of acquisition conditions and limited quantities of CO₂ injected. However, the Monitor 3 (Figure 19.20) and Monitor 4 (Figure 19.21) surveys yield coherent timelapse anomalies when coprocessed with Baseline 2. NRMS maps of the overburden interval show no definite trend indicating good repeatability, whereas in the injection interval the highest NRMS values are in the southeast near where injection well CCS1 is located (Figures 19.20 and 19.21).

Microseismic Monitoring

Microseismicity Pre-CO₂ Injection

Preinjection microseismic activity was monitored by the arrays in CCS1 and GM1 from May 1, 2010 until start of injection on November 15, 2011, during which they recorded more than 68,000 triggered events. Most events were related to surface noise, drilling of the VW1 borehole, well activities, VW1 perforation

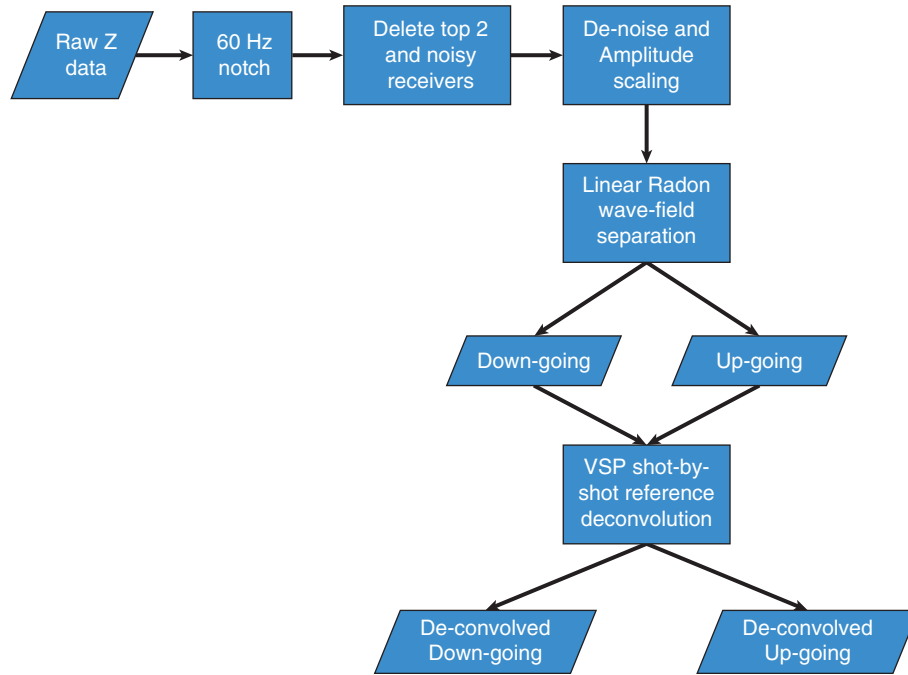


Figure 19.18 Adopted processing flow of single-axis 3D VSP processing.

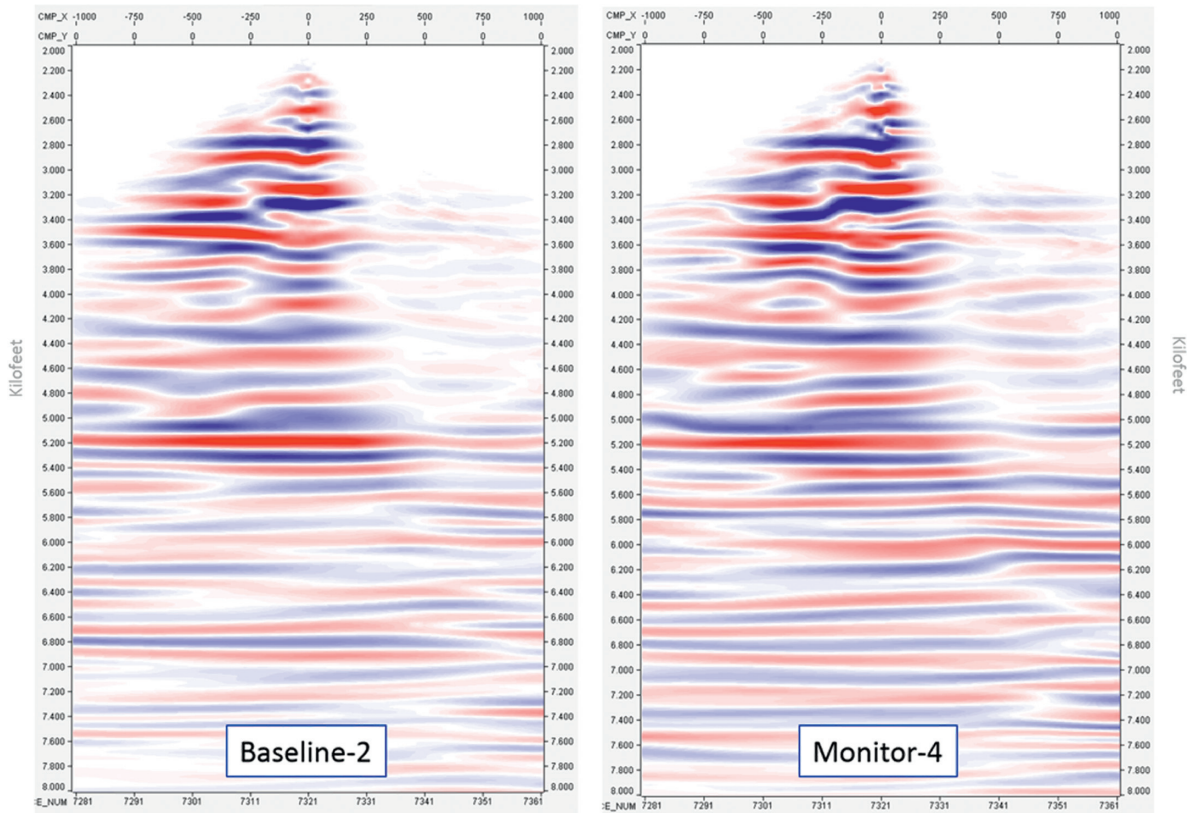


Figure 19.19 Migrated images B2 and M4.

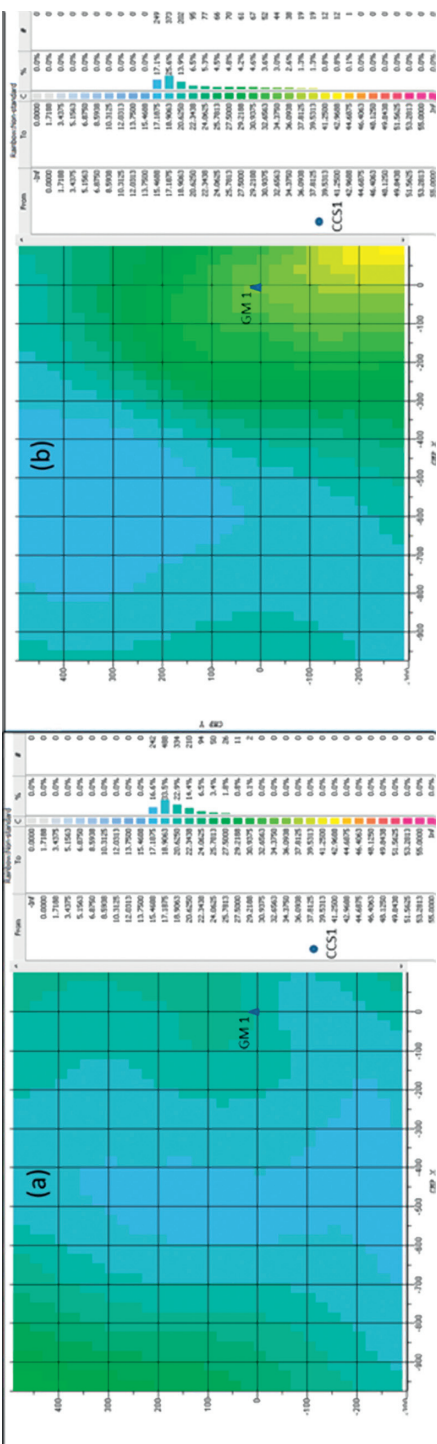


Figure 19.20 Time-lapse NRMS attribute comparison of B2-M3. (a) B2-M3 NRMS attribute in the overburden zone. (b) B2-M3 NRMS in the reservoir.

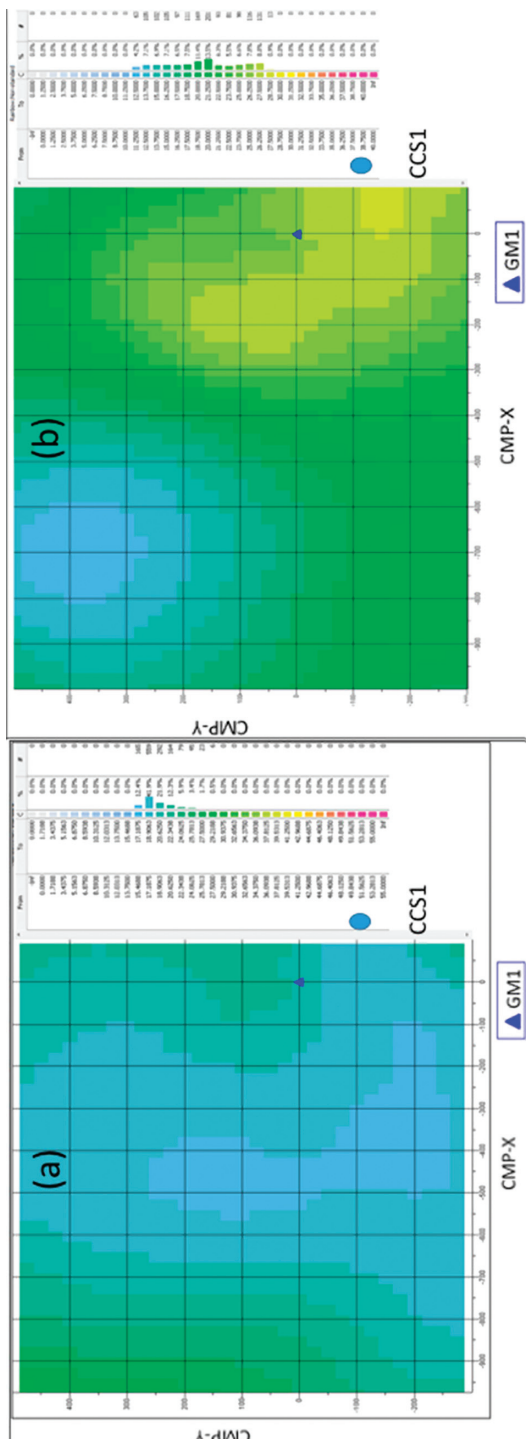


Figure 19.21 Time-lapse NRMS attribute comparison of B2-M4. (a) B2-M4 NRMS attribute in the overburden zone. (b) B2-M4 NRMS in the reservoir zone showing a distinct time-lapse anomaly in the vicinity of the injection well.

shots, and many distant events assumed to be mine blasts because of distance and time of day (8:00 to 17:00). Twenty-one distant natural earthquakes (12 in the United States Geological Survey catalog) and eight local microseismic events were recorded, which appear to be unrelated to well activity and presumed to be background events. These eight background events were located in the Mt. Simon and Argenta; six were located within 457 m of CCS1 and two were located 1646–2408 m from CCS1. The magnitude range for the eight background events was –2.16 to –1.52 (average of –1.83), with a similar range for events related to drilling and well activity of –2.6 to –1.6 (Smith and Jaques, 2016).

Microseismicity during CO₂ Injection

Locatable microseismic events started one month after the start of injection, with two events in December 2011 and 13 in January 2012. During injection, 4848 events were located with an average of four per day having an average magnitude of –0.8. Ninety-four percent of events were less than magnitude 0 but five events were above 1 ranging from 1.01 to 1.17. (The amount of energy released represented by a –1 magnitude is about that of the typical inch long, pencil-thin firecracker.) Using Zoback and Gorelick's (2012) magnitude versus slip surface size and displacement diagram, a magnitude –1 represents a slip of less than a millimeter on a plane of a couple of meters in size to

a slip of a fraction of a tenth of a millimeter on a larger plane of tens of meters.

The range of magnitudes of events is nearly identical in each major geological unit in which events were located: the Precambrian had the highest magnitudes of 1.16 and 1.147, whereas magnitude highs in the mid-to lower 0.8s, were recorded in the Argenta and Mt. Simon, respectively. The lowest moment magnitudes detected in the Precambrian were –2.02 and in the Cambrian sandstones –2.13. The very low magnitudes of microseismic events, their locations and estimated slip plane size, indicate there is little to no risk that induced seismicity at IBDP could cause fault slippage through the caprock and compromise the seal.

About eighty percent of the microseismic events are in the Precambrian crystalline basement, and the remainder in the Mt. Simon and Argenta Formations. The first locatable events were about 600 m from CCS1 and as events continued at this distance, new ones started about 300 m away. Around each of these distances, separate elongated clusters of events began to emerge. Eventually 18 clusters of microseismic events were identified at IBDP, with no correlation existing between time of cluster development and distance from the injection well (Figure 19.22). For example, clusters are numbered in order of appearance, and Cluster 1 averages 548 m from CCS1, Cluster 2 is nearly half that distance (335 m), Cluster 3 averages 457 m, and Cluster 4 averages 823 m from CCS1. Later clusters also

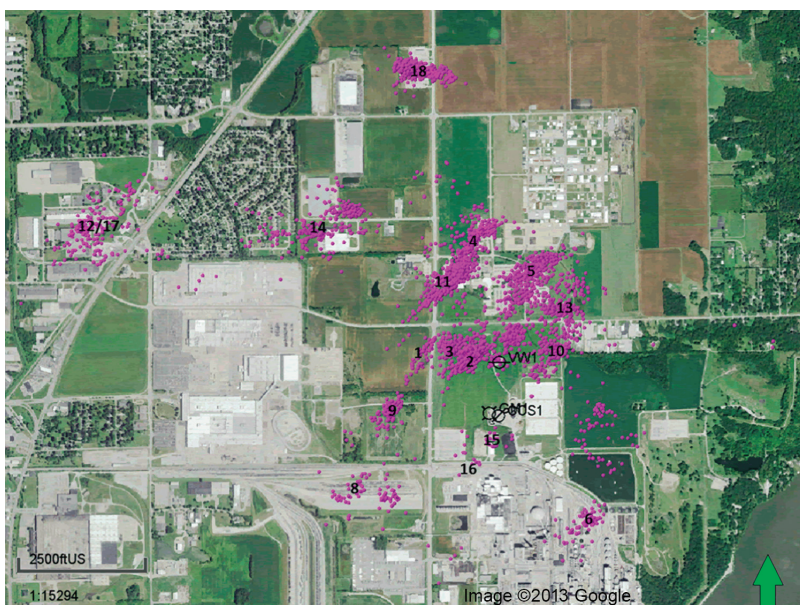


Figure 19.22 Locations of microseismic clusters.

developed out of sequence with increasing distance from the injection well.

Clusters at IBDP continued to add microseismic events during injection and transient shut-in periods, and most developed as an elongated pattern oriented SW–NE. Likely factors other than pore pressure changes influenced the sequence of cluster development, such as the angle of preexisting planes of weakness or defects in relation to maximum horizontal stress direction. Preexisting weak planes or defects close to 30° from the maximum horizontal stress ($S_{H\max}$) direction are optimally oriented in the direction expected for strike-slip movements.

Evidence related to microseismic events induced by hydraulic fracturing suggest they are triggered along

preexisting natural fractures that are favorably oriented for slip (Pearson 1981; Rutledge and Phillips, 2003; Shapiro *et al.*, 2006). Baig *et al.* (2012) observed that with hydraulic fracturing of some horizontal wells events occurred in two main trends: early events were roughly 30° from $S_{H\max}$ and late events were approximately parallel to $S_{H\max}$. Yang *et al.* (2013) found similar trends for hydraulic fracturing in the Bakken formation where detected microseismic events from many stages trend approx. 30° from the direction of $S_{H\max}$. This relation appears to be present at IBDP through the sequence of cluster development, with Cluster 1 at 28° from $S_{H\max}$, Cluster 2 at 11° , Cluster 3 at 9° , and Cluster 4 at 3° (Figure 19.23). The strike of each plane was developed by a best-fit plane through the 3D cloud of

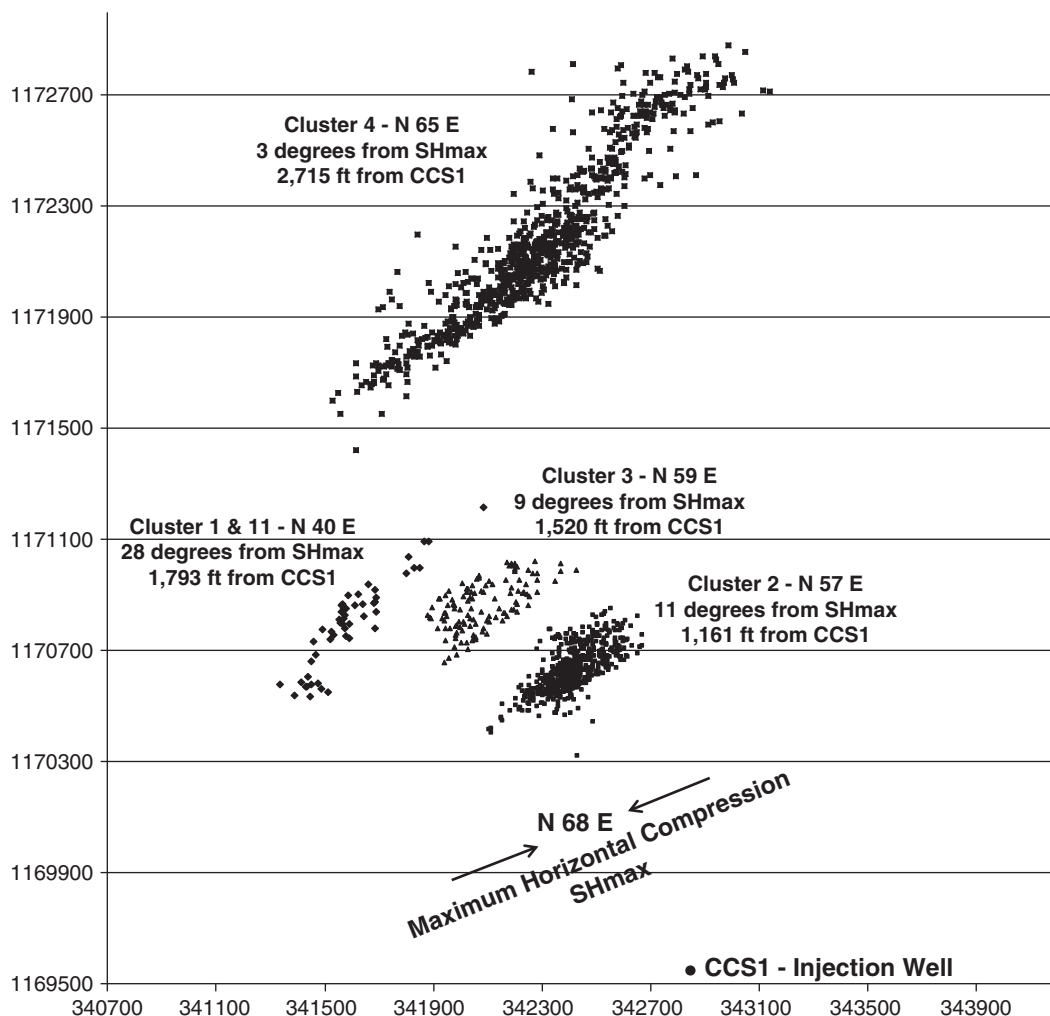


Figure 19.23 Clusters 1–4 directions in relation to maximum horizontal *in situ* stress and average distance from injection well CCS1. Axes are northing and eastings in feet. (From Bauer *et al.*, 2016.)

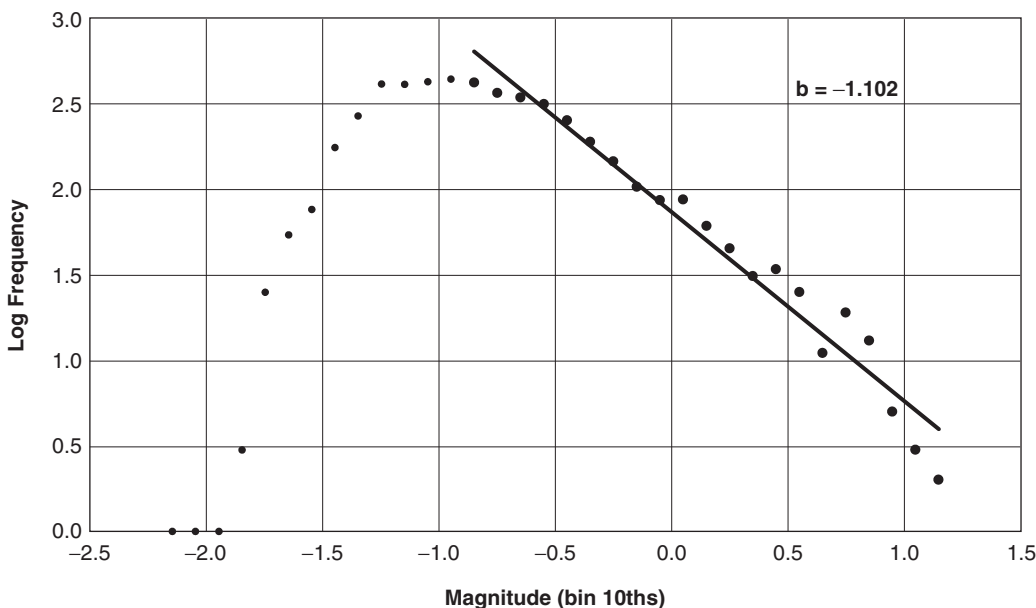


Figure 19.24 Gutenberg–Richter plot of all the microseismicity during the three years of injection. (From Bauer *et al.*, 2016.)

events. The strike of the planes in relation to the *in situ* $S_{H\max}$ fits the first motion analysis indicating right lateral strike-slip motions on many of the clusters (Couëslan *et al.*, 2014). These planes are interpreted to be the reactivation of preexisting features as shown by the Gutenberg–Richter (Gutenberg and Richter, 1956) plots for all the microseismicity, which show b -values close to 1 (Figure 19.24). Will *et al.* (2016b) present an in-depth analysis of the data integration and reservoir response resulting in microseismicity.

The total event population was separated into subsets on the basis of spatial clustering and the fault plane solution (FPS) analysis was performed on individual event subsets. Figure 19.25 shows the FPS result for one of the most developed and coherent event clusters (#4), which exhibits a very good fit to the strike-slip model for an azimuth of N45E. Figure 19.26 shows the FPS superimposed on event clusters.

Monitoring Strategy and Discussion

Integrated Modeling

Each component of the IBDP geophysical program has made a unique contribution to the understanding of key aspects of site characterization such as geological structure, stratigraphy, and reservoir properties dictating well injectivity, storage capacity, and

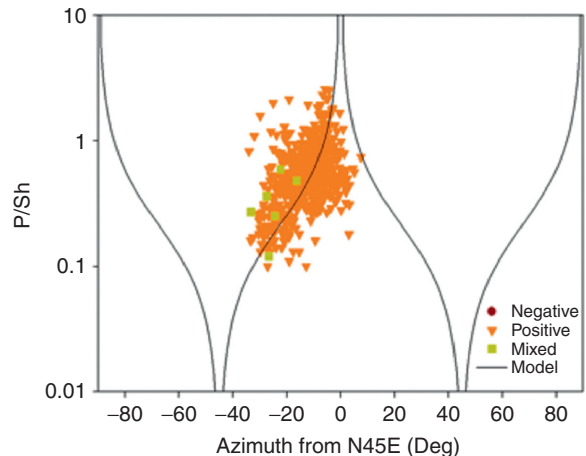
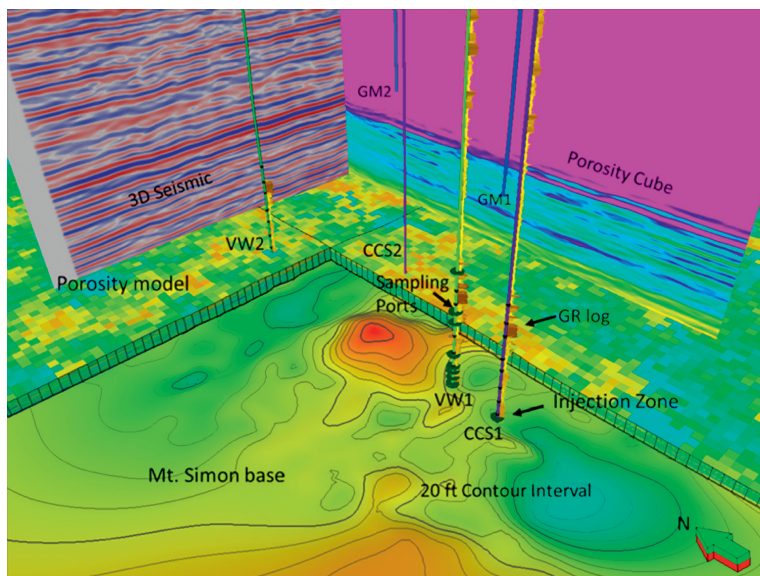
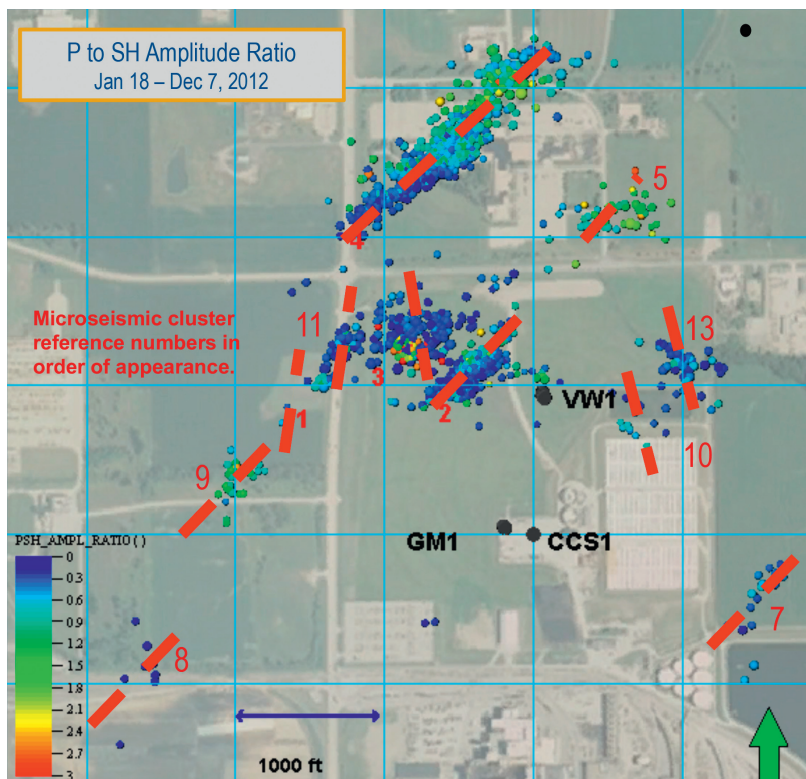


Figure 19.25 FPS for a selected event cluster (#4) using a strike-slip assumption and azimuth.

containment. However, because of intrinsic characteristics such as spatial coverage, resolution, and phenomenological ambiguity, in order to realize its full value, seismic data must be integrated with other direct measurement types such as borehole logs, core, and well tests. Therefore, the IBDP site characterization and monitoring program has included an extensive integrated geologic modeling effort. The various contributions of active seismic methods

Figure 19.26 FPS results for all clusters.**Figure 19.27** Contribution of seismic data to the static geologic model.

to the IBDP geologic model through interpretation of stratigraphic horizons, acoustic impedance and seismic porosity inversion, time-depth domain conversion through integration with acoustic and density well logs, and colocated cokriging of reservoir

properties through integration with petrophysical well logs are shown in Figure 19.27.

Geophysical methods have also been instrumental in monitoring transient (both natural and injection induced) changes within the storage unit as part of the

MVA program. Active and passive seismic measurements, such as time-lapse surveys and passive microseismic monitoring, provide valuable *indirect* measurements of hydrodynamic and mechanical state within the reservoir. However, while these measurements provide valuable information about the timing and location of changes in reservoir state, each on its own is insufficient to yield an unambiguous physical characterization of the responsible phenomena. Characterizing these phenomena requires an understanding of local transient hydrodynamic and stress

state as provided by fluid flow and geomechanical models. Fluid flow and geomechanical models were part of early stage IBDP characterization and have been updated as the project evolves.

The following sections describe the pivotal role of the IBDP integrated model in interpretation of time-lapse seismic and passive monitoring data for understanding of plume development and microseismic mechanisms. The geologic and transient process models have been periodically updated to incorporate new characterization and calibration data (Table 19.6).

Table 19.6 IBDP integrated model development history

	Structure/stratigraphy/ discrete features	Hydrodynamic properties	Use
2008 Preliminary	<ul style="list-style-type: none"> Layer cake stratigraphy defined by well tops from analog well 60 miles away No discrete features 	<ul style="list-style-type: none"> Uniform zonal porosity and permeability Assigned using logs from analog well 60 miles away 	<ul style="list-style-type: none"> Site characterization Basis for initial reservoir simulation model
2010 Update	<ul style="list-style-type: none"> Layer cake stratigraphy: well tops from CCS1 No discrete features 	<ul style="list-style-type: none"> Stochastic zonal porosity and permeability Conditioned to CCS1 well logs 	<ul style="list-style-type: none"> Updated site characterization Basis for initial reservoir simulation plume predictions
2011 Update	<ul style="list-style-type: none"> Stratigraphy: 2010 3D seismic survey and well top control from CCS1 and VW1 No discrete features 	<ul style="list-style-type: none"> Stochastic zonal porosity and permeability Conditioned to CCS1 and VW1 well logs and 2010 seismic inversion products 	<ul style="list-style-type: none"> Update site characterization Basis for final Class VI permit reservoir simulation area of review Basis for preliminary finite element model (FEM)
2013 Update	<ul style="list-style-type: none"> Stratigraphy: 2011 extended 3D seismic survey and well top control from CCS1, VW1, and VW2 Provisional fault interpretation Mechanical features inferred from microseismic data 	<ul style="list-style-type: none"> Stochastic zonal porosity and permeability Conditioned to CCS1, VW1, and VW2 well logs and 2011 seismic inversion products 	<ul style="list-style-type: none"> Update site characterization Basis for updated FEM and preliminary microseismic prediction research
2016 Update	<ul style="list-style-type: none"> Stratigraphy: 2015 seismic survey was completed to be a time-lapse survey for CCS1 injection and baseline survey for CCS2 injection with a 400-m extension to the north 	<ul style="list-style-type: none"> Updated stochastic zonal porosity and permeability based on the additional updated structure Conditioned to CCS2, CCS1, VW1, and VW2 well logs and 2011 seismic inversion products 	<ul style="list-style-type: none"> Update site characterization for reservoir simulations

Contributions include stratigraphic horizons, seismic porosity inversion, and collocated–cokriged reservoir properties.

Mapping the CO₂ Plume

Injection of CO₂ produces variations in elastic properties in the reservoir that change the time-lapse seismic response; these changes are often subtle and are nonunique with respect to saturation and pressure effects. At the IBDP, a “simulation-to-seismic” workflow has been used for model based integration of time-lapse seismic data and direct measurements of reservoir state using the geological and reservoir simulation models developed for site characterization and plume predictions.

The reservoir model was calibrated to injector and multilevel monitoring well pressures to compute the isotropic effective elastic properties for the reservoir at the times of seismic surveys. Thermodynamic properties for brine were computed using Batzle–Wang equations (Batzle and Wang, 1992), and CO₂ properties were computed using new analytical expressions in the National Institute of Standards and Technology Reference Fluid Thermodynamic and Transport Properties Database (NIST–REFPROP) software. An average of Hashin–Shtrikman (H–S) bounds were used to calculate the bulk and shear moduli of solid rock using rock compositions derived from elemental analysis on available logs. Effective elastic properties of a fluid-filled formation were computed using

Gassmann fluid substitution model and used to forward model attribute differences corresponding to field survey times.

Before time-lapse integration, the calibrated reservoir simulation model predicted an approximately radial plume centered on the injection well (Senel *et al.* 2014). This simulation was calibrated to 15 months of injection and monitoring well pressure and verified with pulse neutron logs. Upon extraction of time-lapse attributes (Figures 19.15–19.17) from the 2011–2015 surface seismic survey pair, a significant discrepancy was noted in the shape and extent of the current plume prediction and time-lapse observation. While differences are expected owing to vertical plume geometry and seismic detection limits, the significant deviation in aerial geometry (in particular the truncation of northward plume migration) indicated fundamental deficiencies in the simulation model. Examining the 2011 survey through seismic attribute and inversion analysis revealed that features exist in the baseline seismic data suggestive of enhanced reservoir quality and a possible flow barrier having geometrical characteristics consistent with the time-lapse anomaly. These features were not incorporated in the original model due to use of a global interpolation scheme. In an updated model, the reservoir quality was modified and a hypothetical flow barrier was inserted corresponding to the features identified in Figure 19.28. Figure 19.29 shows the resulting simulated plume and forward modeled time-lapse acoustic impedance change along with

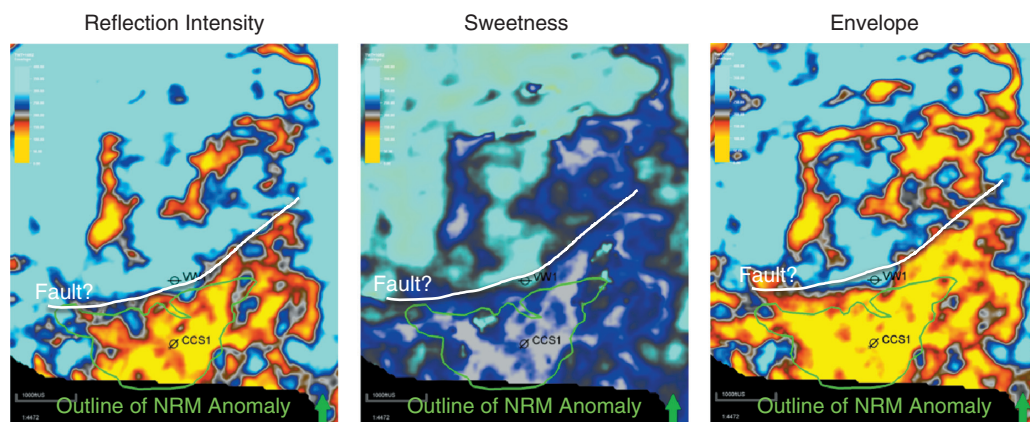


Figure 19.28 Seismic attributes used as the basis for modification of the reservoir model for time-lapse seismic history matching. (From Will *et al.*, 2017.)

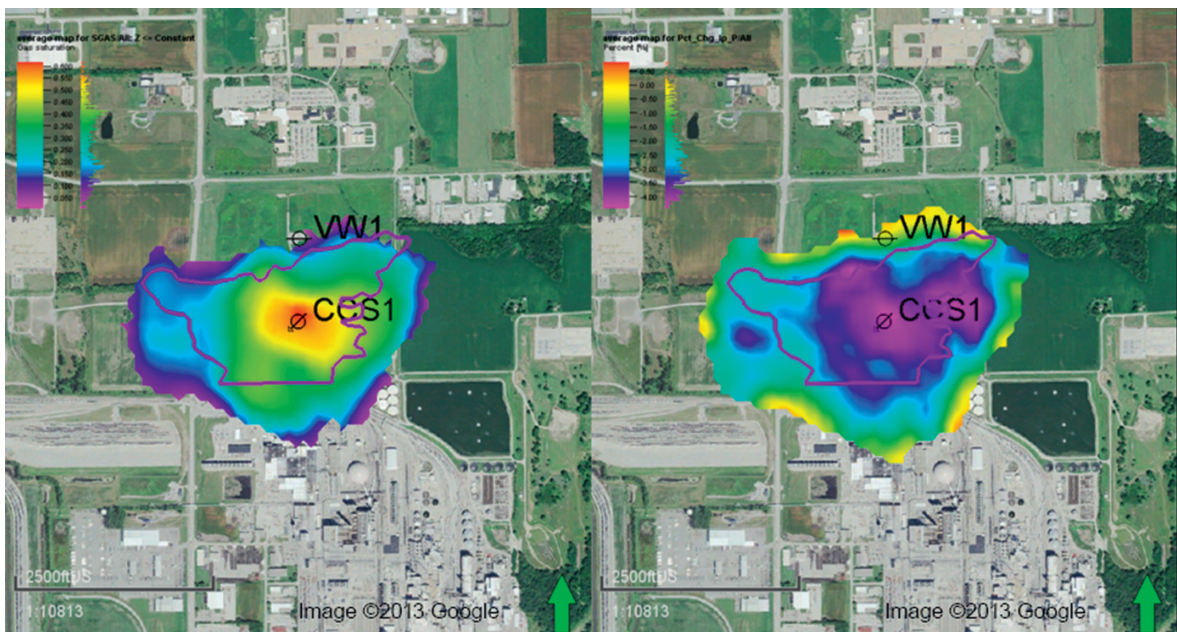


Figure 19.29 Plume simulation and forward-modeled acoustic impedance change. (Left) Aerial view of simulated 2015 monitor CO₂ plume and outline of 2001–2015 surface seismic time-lapse NRM attribute (from Figure 19.17). (Right) Aerial view of forward modeled time-lapse acoustic impedance change and outline of 2001–2015 surface seismic time-lapse NRM attribute. (From Will et al., 2017.)

the outline of the NRM anomaly (from Figure 19.17) in which discrepancies have been greatly reduced. Qualitative analysis of this new result suggests a detectability limit of approx. 3–4% change in acoustic impedance. Similar efforts are being deployed toward addressing saturation inversion.

Summary

Integrating geophysical and geological data is necessary to develop robust geological, fluid flow, and geomechanical models, and to provide essential support for feasibility assessment, operational planning, and regulatory compliance. The IBDP demonstrates practical application of existing acquisition and analytical geophysical methods to achieve the goals of a large-scale CO₂ storage demonstration project. Seismic geophysical methods comprise an extensive set of tools that may be used to fulfill many site characterization and monitoring objectives for regulatory compliance or scientific investigations. Data acquisition techniques may be tailored for the operational environment and the specific imaging objective throughout the life of a CO₂ storage project from pre-drill site selection to plume monitoring

during and after injection. Sophisticated noise attenuation and imaging data processing techniques help to overcome many of the challenges encountered in typical operational scenarios, providing input to structural interpretation, reservoir property estimation, and monitoring. Geophysical monitoring and analysis of the IBDP will continue throughout the postinjection and postinjection site care compliance monitoring phase (expected end date 2020).

References

- Baig, A. M., Urbancic, T., and Viegas, G. (2012). Do hydraulic fractures induce events large enough to be felt on surface? *CSEG Recorder*, 10(October 2012): 40–46.
- Batzle, M., and Wang, Z. (1992). Seismic properties of pore fluids. *Geophysics*, 57: 1396–1408.
- Bauer, R. A., Carney, M., and Finley, R. J. (2016). Overview of microseismic response to CO₂ injection into the Mt. Simon saline reservoir at the Illinois Basin-Decatur Project. *International Journal of Greenhouse Gas Control*, 54(1): 378–388.
- Couëslan, M. L., Leetaru, H. E., Brice, T., Leaney, W. S., and McBride, J. H. (2009). Designing a seismic program for

- an industrial CCS site: Trials and tribulations. *Energy Procedia*, **1**(1): 2193–2200.
- Couëslan, M. L., Ali, S., Campbell, A., et al. (2013). Monitoring CO₂ injection for carbon capture and storage using time-lapse 3D VSPs. *Leading Edge*, **32**(10): 1268–1276.
- Couëslan, M. L., Butsch, R., Will, R., and Locke, R. A. II (2014). Integrated reservoir monitoring at the Illinois Basin–Decatur Project. *Energy Procedia*, **63**: 2836–2847.
- Freiburg, J. T., Morse, D. G., Leetaru, H. E., Hoss, R. P., and Yan, Q. (2014). A depositional and diagenetic characterization of the Mt. Simon Sandstone at the Illinois Basin–Decatur Project carbon capture and storage site, Decatur, Illinois, USA, Illinois State Geological Survey Circular 583.
- Greenberg, S. G., Bauer, R., Will, R., et al. (2017). Geologic carbon storage at a one million tonne demonstration project: Lessons learned from the Illinois Basin–Decatur Project. *Energy Procedia*, **114**: 5529–5539.
- Gutenberg, B., and Richter, C. F. (1956). Magnitude and energy of earthquakes. *Annals of Geophysics*, **9**(1): 1–15.
- Haimson, B. Z., and Doe, T. W. (1983). State of stress, permeability, and fractures in the Precambrian granite of Northern Illinois. *Journal of Geophysical Research*, **88**(B9): 7355–7371.
- Leetaru, H. E., and Freiburg, J. T. (2014). Litho-facies and reservoir characterization of the Mt Simon Sandstone at the Illinois Basin–Decatur Project. *Greenhouse Gases: Science and Technology*, **4**(5): 580–595.
- Leetaru, H. E., and McBride, J. H. (2009). Reservoir uncertainty, Precambrian topography, and carbon sequestration in the Mt. Simon Sandstone, Illinois Basin. *Environmental Geosciences*, **16**(4): 235–243.
- Palkovic, M. (2015). *Depositional characterization of the Eau Claire Formation at the Illinois Basin–Decatur Project: Facies, mineralogy and geochemistry*. M.S. thesis, University of Illinois at Urbana-Champaign.
- Pearson, C. (1981). The relationship between microseismicity and high pore pressures during hydraulic stimulation experiments in low permeability granitic rocks. *Journal of Geophysical Research*, **86**: 7855–7864.
- Rutledge, J. T., and Phillips, W. S. (2003). Hydraulic stimulation of natural fractures as revealed by induced microearthquakes, Carthage Cotton Valley gas field, east Texas. *Geophysics*, **86**(2): 441–452.
- Senel, O., Will, R. and Butsch, R. J. (2014). Integrated reservoir modeling at the Illinois Basin–Decatur Project. *Greenhouse Gases: Science and Technology*, **4**(5): 662–684.
- Shapiro, S. A., Dinske, C., and Rothert, E. (2006). Hydraulic-fracturing controlled dynamics of microseismic clouds. *Geophysical Research Letters*, **33**: L14312.
- Smith, V., and Jaques, P. (2016). Illinois Basin–Decatur Project pre-injection microseismic analysis. *International Journal of Greenhouse Gas Control*, **54**(1): 362–377.
- Will, R., El-Kaseeh, G., Jaques, P., Carney, M., Greenberg, S., and Finley, R. (2016a). Microseismic data acquisition, processing, and event characterization at the Illinois Basin–Decatur Project. *International Journal of Greenhouse Gas Control*, **54**(1): 404–420.
- Will, R., Smith, V., Lee, D., and Senel, O. (2016b). Data integration, reservoir response, and application. *International Journal of Greenhouse Gas Control*, **54**(1): 389–403.
- Will, R., El-Kaseeh, G., Leetaru, H., Greenberg, S., Zaluski, W., and Lee S.-Y. (2017). Quantitative integration of time lapse seismic data for reservoir simulator calibration: Illinois Basin–Decatur Project. Carbon Capture, Utilization & Storage Conference, Chicago, IL, April 10–13.
- Yang, Y., Zoback, M., Simon, M., and Dohmen, T. (2013). An integrated geomechanical and microseismic study of multi-well hydraulic fracture stimulation in the Bakken Formation. SPE paper 168778 presented at the Unconventional Resources Technology Conference, Denver, CO, August 12–14.
- Zoback, M. D., and Gorelick, S. M. (2012). Earthquake triggering and large-scale geologic storage of carbon dioxide. *Proceedings of the National Academy of Sciences of the USA*, **109**(26): 10,164–10,168.

